potential of -1.1 V. The application of either a cathodic or anodic potential can be expected to cause the hydrogen embrittlement or anodic dissolution mechanism to dominate. The necked region of D54S tested at the free corroding potential and at 0.0 V are shown in Figures 3.11 and 3.12, respectively. Significant intergranular surface cracking may be observed in Figure 3.12.

3.3.4 Conclusions

The initial evaluation of three accelerated SCC test methods: the notched rod load relaxation, the electrochemical acceleration, and the slow strain rate tests, indicated that the slow strain rate test was the most promising.

The slow strain rate test provides a rapid, reliable and reproducible assessment of susceptibility to SCC as a function of heat treatment for the alloy system tested. The results are further consistent with service experience of the alloys. It is expected that the test will not only lend itself to the demands of an alloy development research project, but also to routine testing in a production environment.

Reduction in area proved to be the most sensitive ductility parameter, providing a ductility ratio approaching unity for alloy and temper conditions not susceptible to SCC. Decreasing ratios imply increasing susceptibility to SCC.

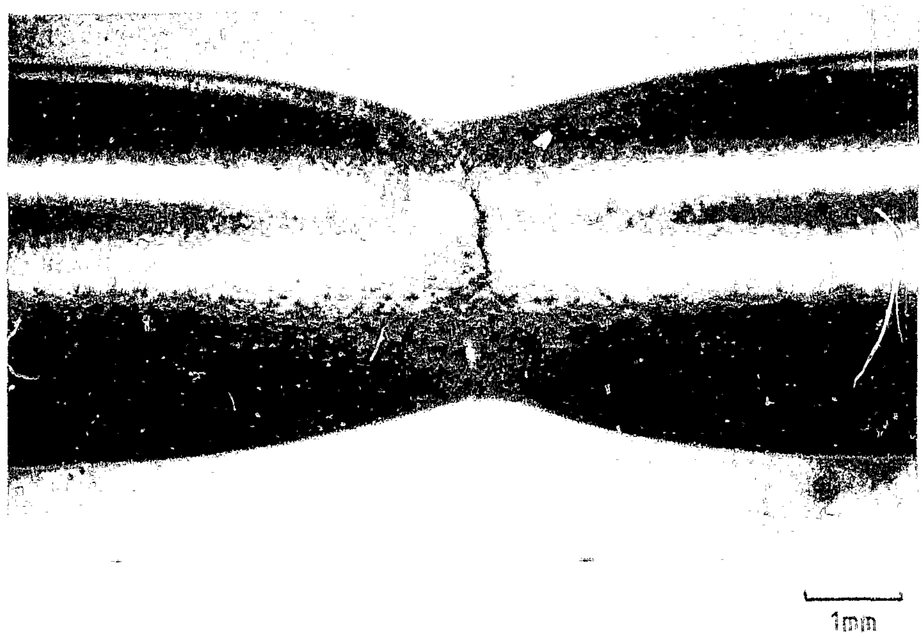

Figure 3.11 Necked region of D54S at free corroding potential

Figure 3.12 Necked region of D54S at the anodic potential of 0.0V

Particularly in combination with an applied electrochemical potential, the slow strain rate test is capable of providing useful information for mechanistic studies of SCC.

3.4 The Effect of Heat Treatment Variables on SCC

The effects of final ageing time and temperature, and quench rate from solution heat treatment, on susceptibility to SCC have been investigated using the slow strain rate SCC test method. The investigation was also intended to reveal any relationship between susceptibility to SCC and variations of some microstructural feature.

3.4.1 Experimental Procedure

Susceptibility to SCC as a function of the final ageing time and temperature was determined by testing nine D74S plate sections in different temper conditions. Preparation of the material has been described in Section 2.4.5. Final ageing times between 6 and 48 hours (at 135°C), and 2 to 48 hours (at 160°C) were used. The final ageing schedules have already been given in Table VII (Section 2.4.5).

The effect of quench rate on resistance to SCC was assessed by testing six D74S plate sections quenched at rates varying from 175 $K.s^{-1}$ to 0.009 $K.s^{-1}$. The

Particularly in combination with an applied electrochemical potential, the slow strain rate test is capable of providing useful information for mechanistic studies of SCC.

3.4 The Effect of Heat Treatment Variables on SCC

The effects of final ageing time and temperature, and quench rate from solution heat treatment, on susceptibility to SCC have been investigated using the slow strain rate SCC test method. The investigation was also intended to reveal any relationship between susceptibility to SCC and variations of some microstructural feature.

3.4.1 Experimental Procedure

Susceptibility to SCC as a function of the final ageing time and temperature was determined by testing nine D74S plate sections in different temper conditions. Preparation of the material has been described in Section 2.4.5. Final ageing times between 6 and 48 hours (at 135°C), and 2 to 48 hours (at 160°C) were used. The final ageing schedules have already been given in Table VII (Section 2.4.5).

The effect of quench rate on resistance to SCC was assessed by testing six D74S plate sections quenched at rates varying from 175 $K.s^{-1}$ to 0.009 $K.s^{-1}$. The material was peak aged after quenching. Details of the quench rates and final ageing schedule were described in Section 2.4.5.

Slow strain rate SCC testing was conducted according to the procedure described in Section 3.3.3. Four long transverse round tensile specimens were prepared from all plate sections in order to conduct two SCC tests in both inert and corrosive environments. The mean value is quoted for each case.

Resistance to SCC is expressed as a ductility ratio. The ductility parameter used is the reduction of area of the necked region. Variations of microstructural features, particularly the PFZ width, were obtained from the CTEM studies reported in Section 2.4.6.

3.4.2 Results

The results of the slow strain rate tests as a function of ageing time and temperature are shown in Figures 3.13 and 3.14, for ageing temperatures of 135 and 160°C, respectively. Vickers hardness measurements are included as an indication of mechanical properties.

The major microstructural variation observed with ageing time and temperature was found to be the PFZ width. A relationship was apparent between the PFZ width during final ageing and resistance to SCC. This linear relationship is shown for each final ageing temperature in Figure 3.15.

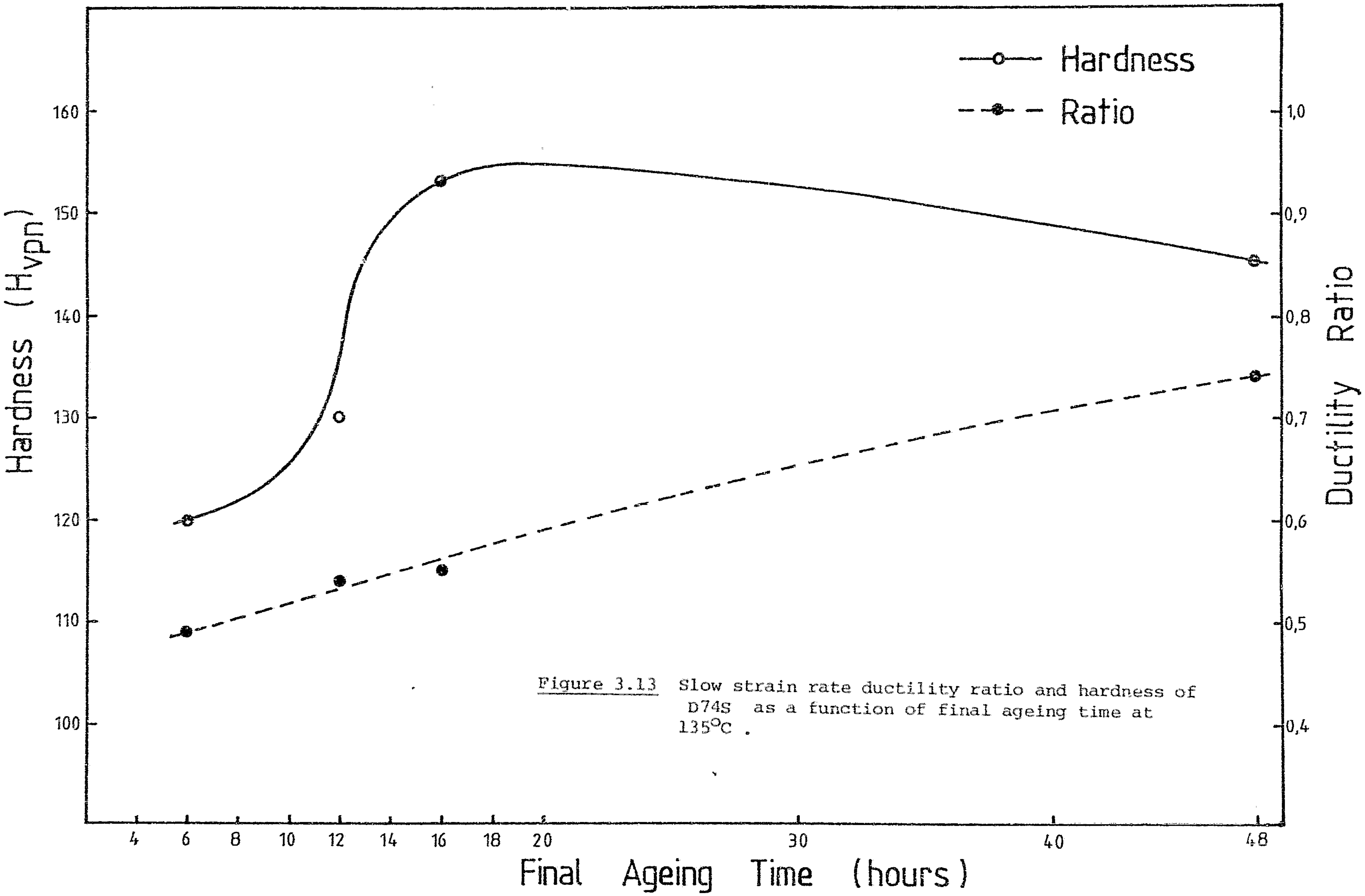

Figure 3.13 Slow strain rate ductility ratio and hardness of D74S as a function of final ageing time at 135°C .

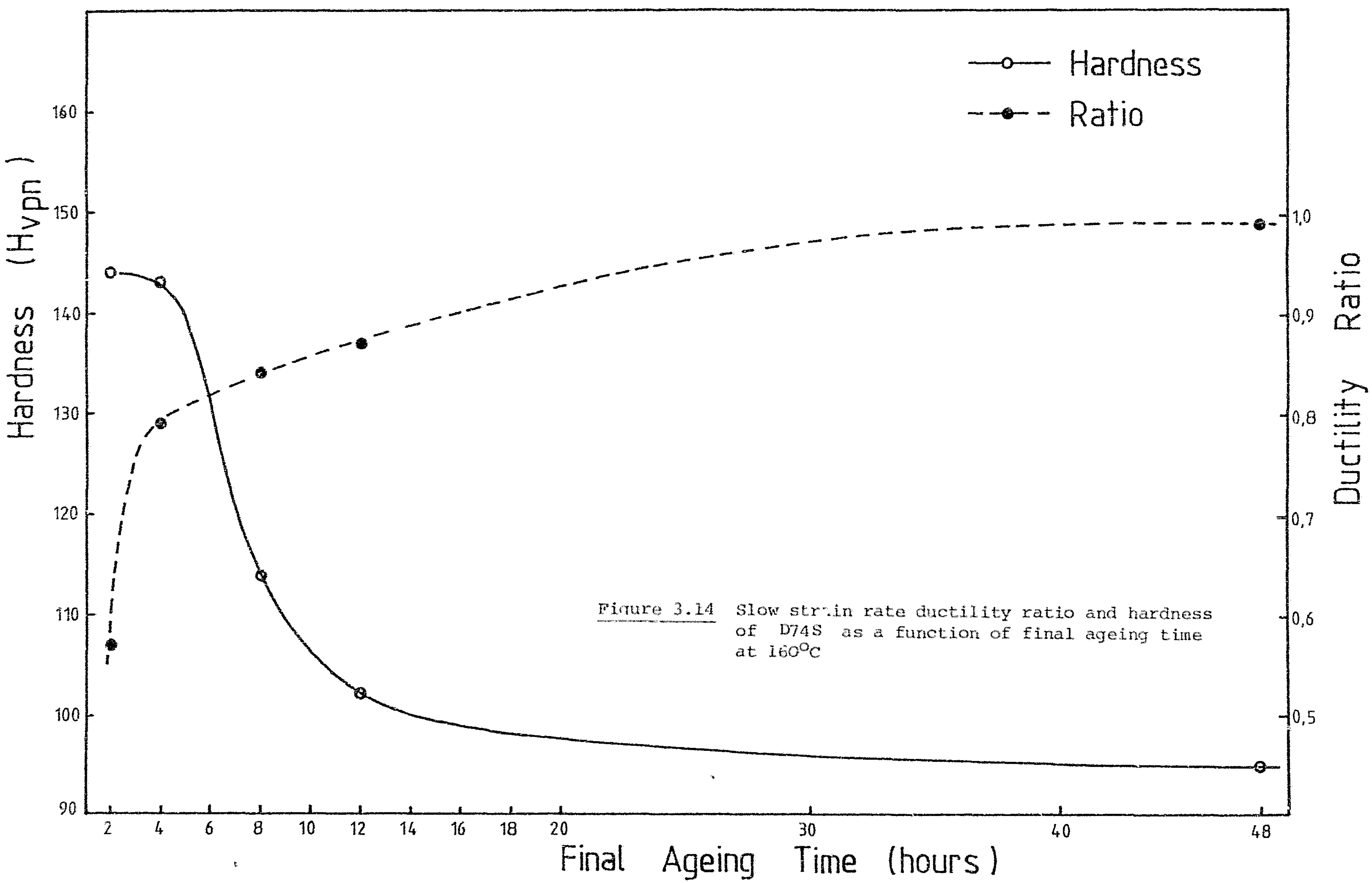

Figure 3.14 Slow strain rate ductility ratio and hardness of D74S as a function of final ageing time at 160°C

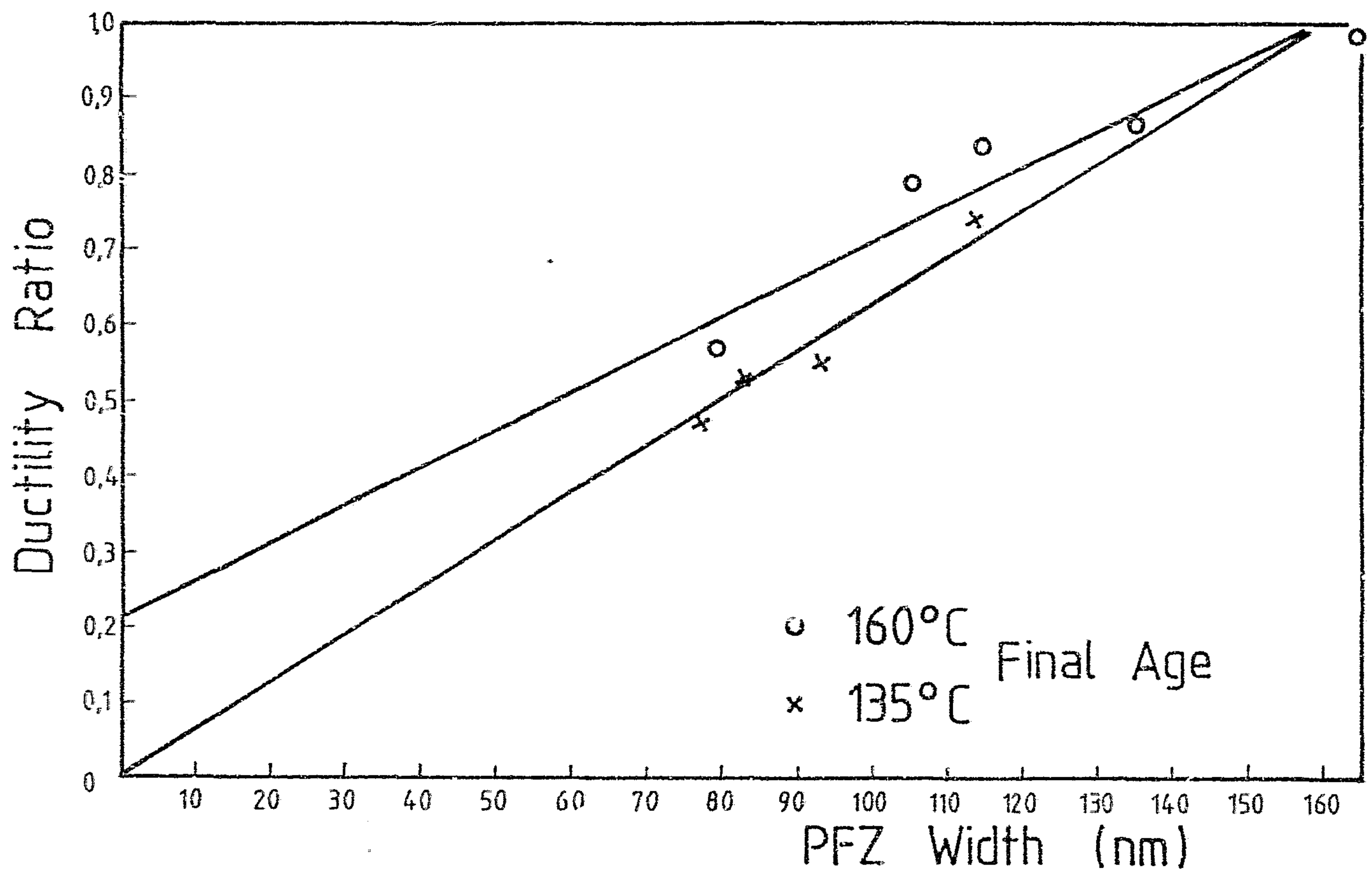

Figure 3.15 The effect of PFZ width produced by different final ageing times on the ductility ratio obtained from SCC testing

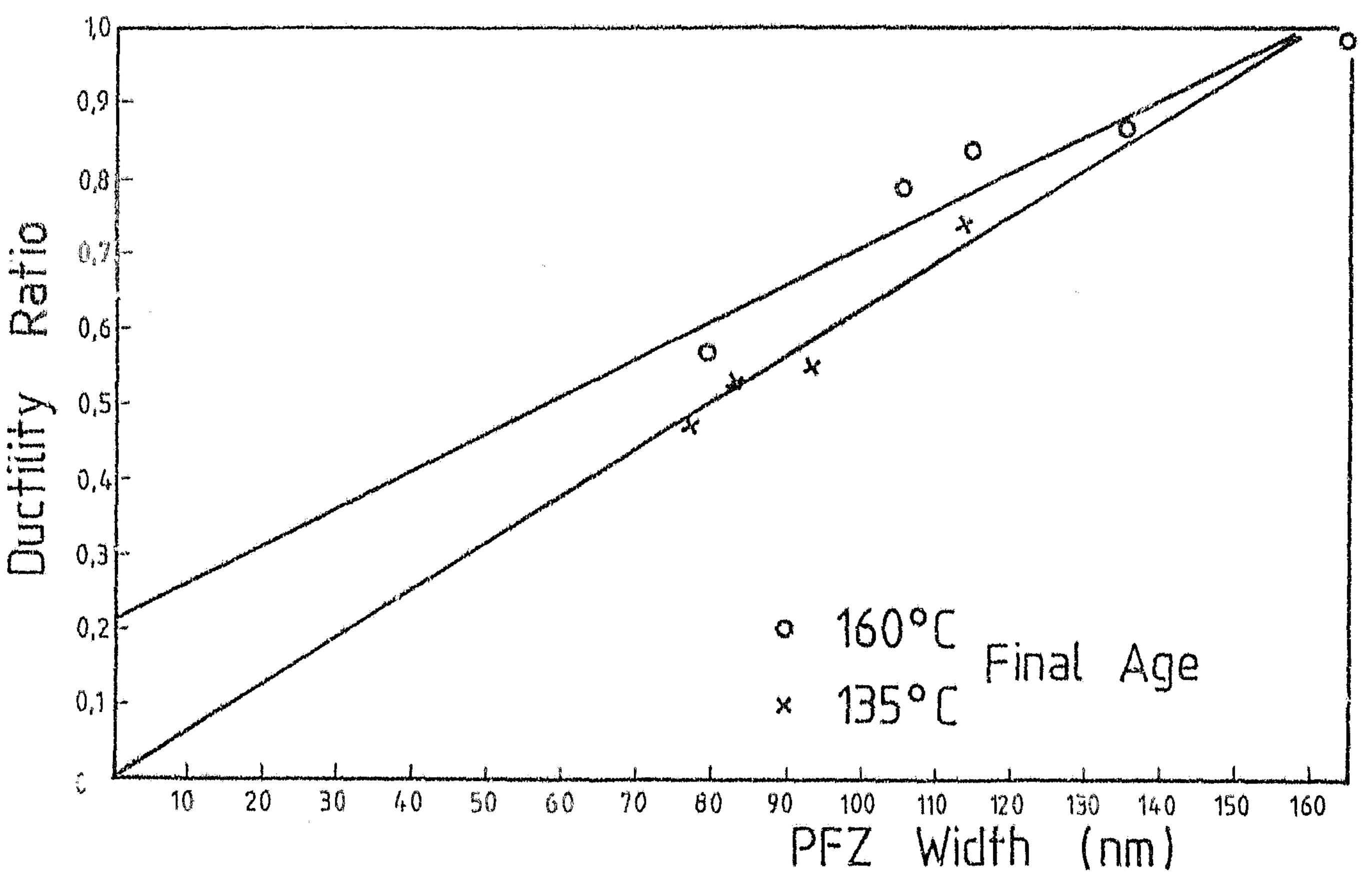

Figure 3.15 The effect of PFZ width produced by different final ageing times on the ductility ratio obtained from SCC testing

The results for material quenched at different rates is shown in Figure 3.16. The quench rates have been plotted on a logarithmic axis. Vickers hardness values are again included as a measure of mechanical properties.

The PFZ width is plotted as a function of the ductility ratio in Figure 3.17. The PFZ width at the lowest quench rate is obtained by extrapolating the curve of quench rate versus PFZ width in Figure 2.55.

3.4.3 Discussion

The characteristic increase in resistance to SCC by overageing a typical Al-Zn-Mg alloy, was observed at both final ageing temperatures (Figures 3.13 and 3.14). The 160°C final age results in a rapid overageing effect (within the first 12 hours) which is accompanied by a corresponding rapid increase in resistance to SCC. The 135°C final age shows a more gradual increase in resistance to SCC. It appears, however, that increased resistance is only achieved with a considerable and unacceptable loss of properties (Figure 3.14).

Overaging had little effect on the ductility as measured by reduction in area for specimens tested in the inert environment. No definite trend was obvious with final ageing time, or indeed final ageing temperature. Under these conditions it may be possible to reduce the number of inert slow strain rate tests performed in future studies, therefore reducing the total testing time substantially.

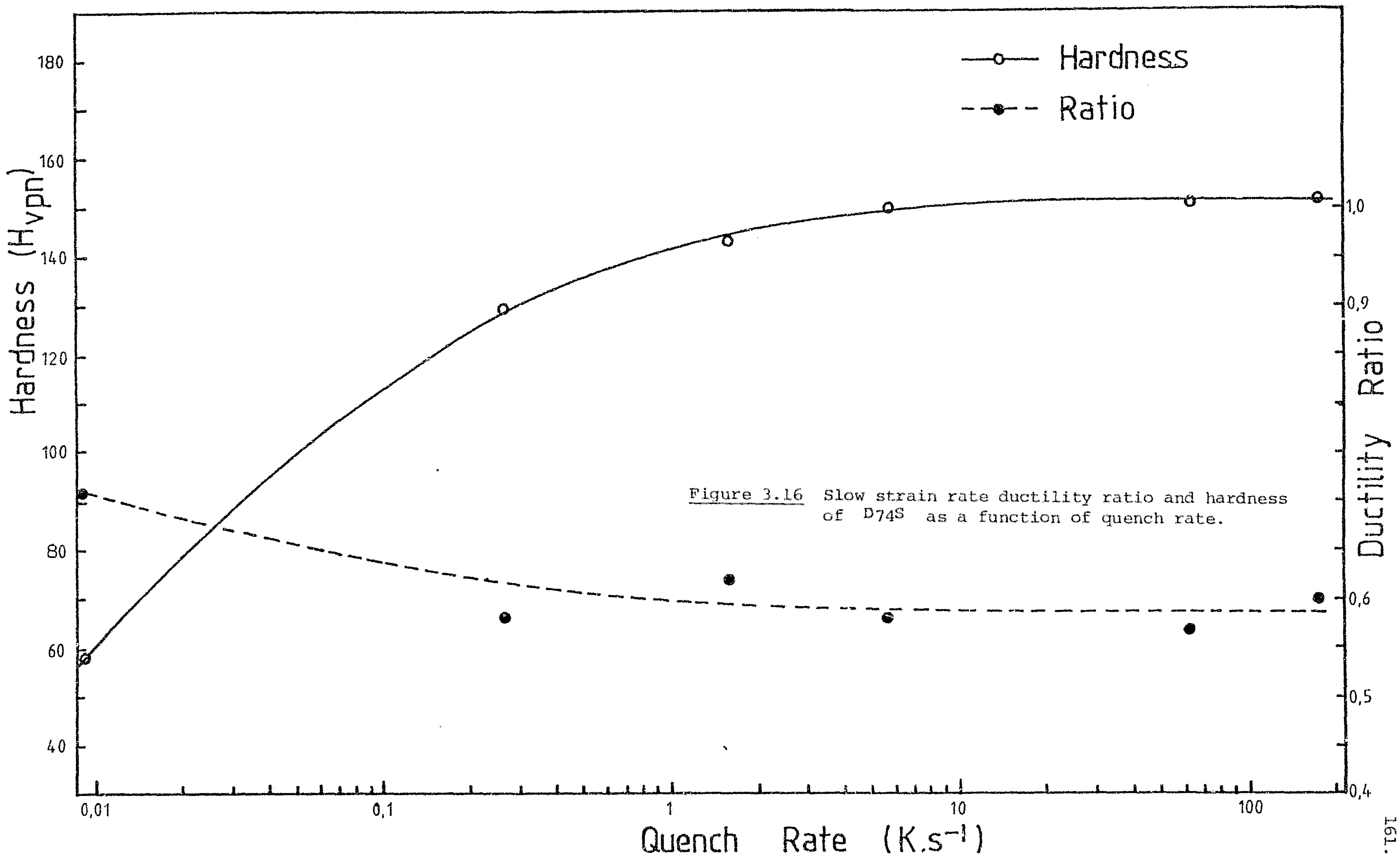

Figure 3.16 Slow strain rate ductility ratio and hardness of D74S as a function of quench rate.

It is clear from Figure 3.15 that a linear relationship exists between the PFZ width during final ageing and susceptibility to SCC. The results, however, do not conclusively prove that the increase in PFZ width is the primary cause of increased resistance to SCC. Growth of the PFZ width depends on bulk diffusion of solute atoms at the elevated ageing temperature. The same mechanism is responsible for the formation of a solute profile at the grain boundary. It seems more likely, in the light of current SCC theories (Section 3.2), that the PFZ width varies at the same rate and could, therefore, merely be a secondary indication of the solute profile which is developed during ageing.

The observed moderate decrease in susceptibility with decreasing quench rate (Figure 3.16) is in agreement with that established for weldable 7000 series alloys (Section 2.4.3). It does not appear, however, that substantial increases in resistance to SCC may be achieved in D74S-type alloys by employing reduced quench rates.

Non-weldable Cu-containing Al-Zn-Mg alloys are known to show improved resistance to SCC at rapid quench rates (Section 2.4.3). It appears therefore that the Cu content of D74S (0.25% max) is sufficient to produce borderline behaviour between non-Cu and Cu-containing alloys. This argument is further corroborated by the similar moderate increase in resistance to SCC shown by an Al-Zn-Mg alloy containing 0.16% Cu which has been investigated by Cordier, et al.[15] (Section 2.2.2, Figure 2.10).

A clear relationship does not appear to exist between the PFZ width obtained from different quench rates and the susceptibility to SCC (Figure 3.17). Although the PFZ width has been substantially increased with reduced quench rates, the susceptibility to SCC remains essentially unchanged. The use of reduced quench rates, however, would also lead to an increasing solute concentration profile at the grain boundaries. An explanation is therefore required to explain why an increasing solute concentration profile produced by quenching has little effect on SCC resistance, while that developed during overageing leads to a marked improvement. The results of these preliminary tests are not sufficiently detailed with respect to the operative mechanisms. However, it is possible to propose a tentative explanation for some of the observed effects, in terms of the influence of the small Cu addition.

The anodic tendency of aluminium is increased by the addition of Mg and particular Zn (as discussed in Section 3.2.2). Cu additions, however, increase the cathodic tendency of the alloy. The effect, therefore, of either decreasing the Zn concentration in the grain boundary region, or increasing the Cu concentration will be to decrease the anodic potential relative to the remainder of the microstructure. SCC will therefore be reduced by the suppression of the anodic dissolution mechanism (Section 3.2.2).

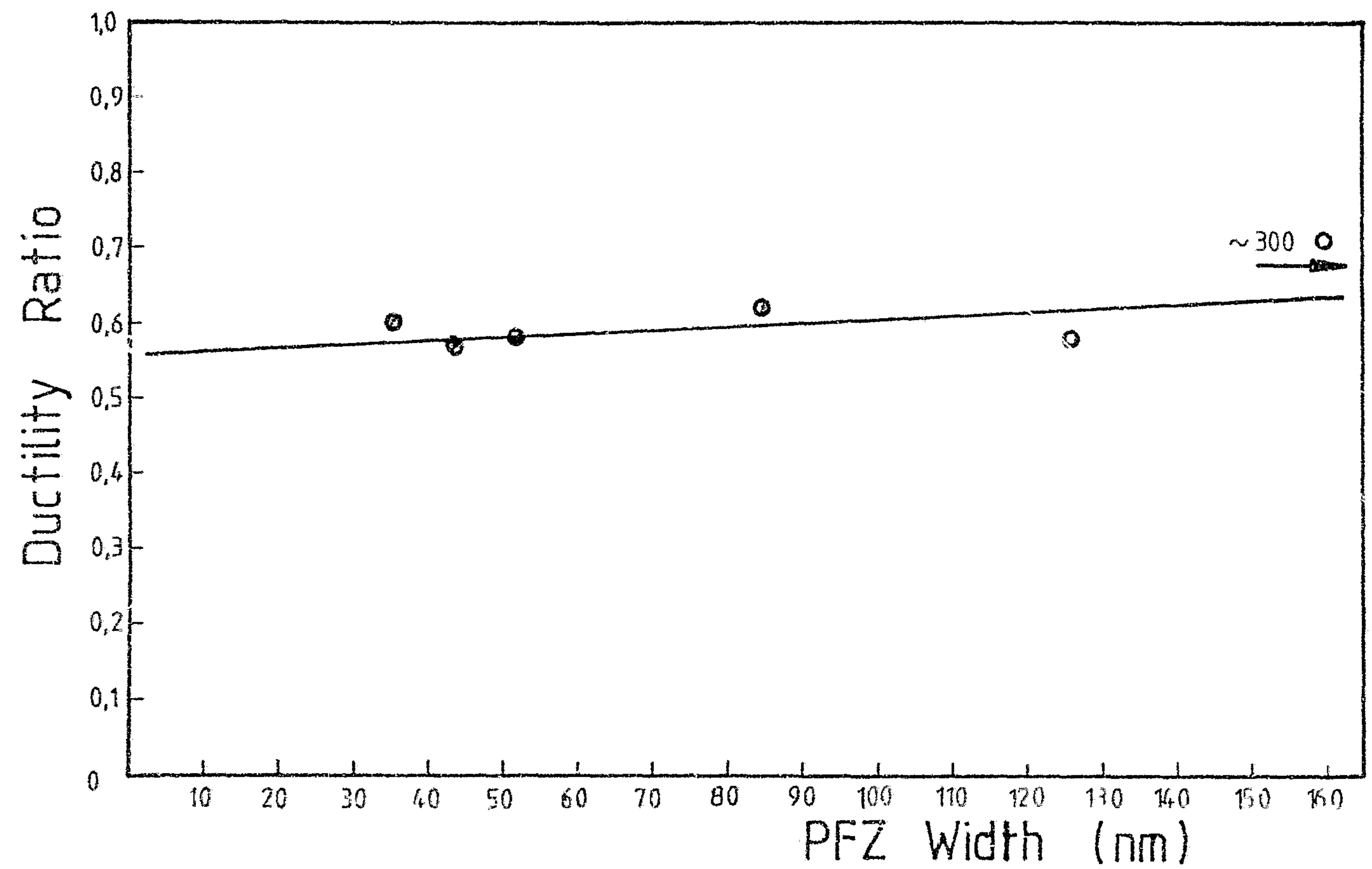

Figure 3.17 The effect of PFZ width produced by different quench rates on the ductility ratio obtained from SCC testing.

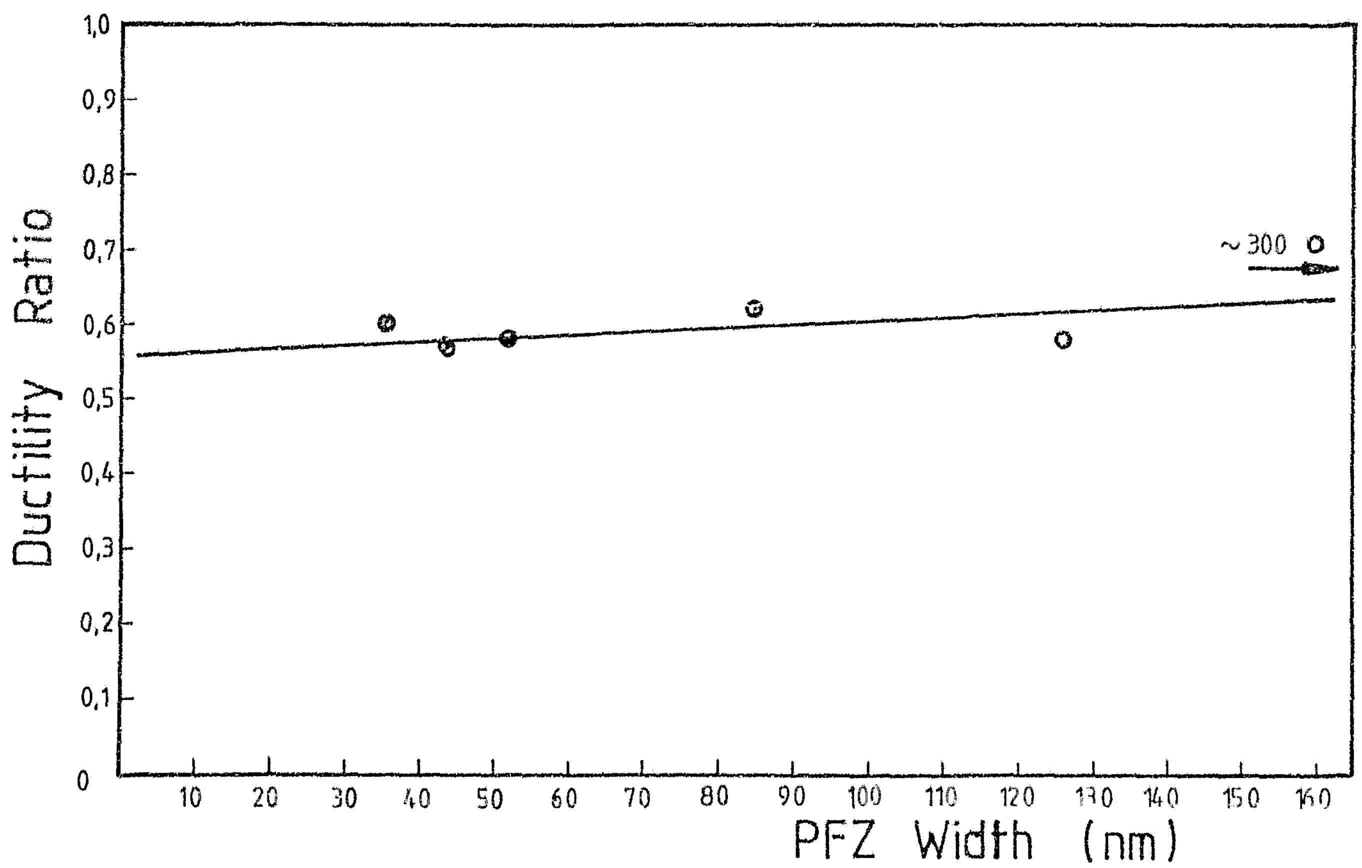

Figure 3.17 The effect of PFZ width produced by different quench rates on the ductility ratio obtained from SCC testing.

The addition of 0.16% Cu to an Al-5Zn-1.7Mg alloy (containing 0.15% Cr) only improves SCC resistance at faster quench rates[15], (see Figure 3.18 which compares Figures 2.6 (2) and 2.10 (2) in Section 2.2.2). Considering the alloy with no Cu-addition, an increasingly large solute (Zn, Mg) profile is developed at grain boundaries with decreasing quench rates, resulting in improved resistance to SCC. At fast quench rates, a small profile is developed which does not sufficiently reduce the anodic potential of the grain boundary, and leads to the poor resistance to SCC.

Small additions of Cu do not appear to reduce the susceptibility to SCC at low quench rates. It has been shown[67] that depletion of the solution Cu concentration takes place at the grain boundary with overageing. A similar depletion of Cu must therefore also occur for reduced quench rates. At low quench rates the effect of the large (Zn, Mg) solute concentration profile on the anodic potential of the grain boundary is dominant and little affected by the presence of Cu (which is itself depleted at the grain boundary). The susceptibility to SCC thus remains unchanged. However, at high quench rates, depletion of Cu at grain boundary regions is not expected to occur. The cathodic tendency of the Cu will therefore decrease the anodic potential of the grain boundary to an increasing extent with increasingly rapid quench rates. SCC is therefore improved at fast quench rates.

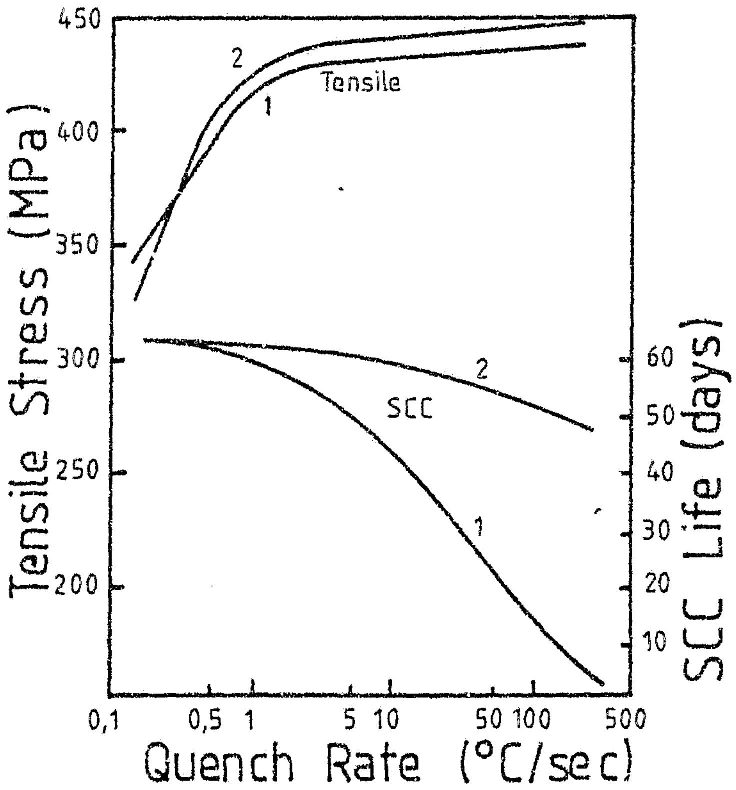

Figure 3.18 The effect of quench rate on the tensile properties and SCC test life spans for:
(1) Al-5 Zn- 1.7 Mg + 0.15 Cr
(2) Al-5 Zn- 1.7 Mg + 0.15 Cr + 0.16 Cu

The above mechanism can only be expected to operate for small Cu-additions, where the effects of the addition itself and the solute profile on the anodic potential of the grain boundary are similar.

In D74S type alloys it appears possible, using different quench rates, to vary the solute profile and PFZ width independently of the susceptibility to SCC (Figure 3.17). This is not possible, however, during the final ageing process (Figure 3.15). In this case, after fast quenching from solution heat treatment, improvements in resistance to SCC are still possible by further depletion of solute at the grain boundaries during overageing.

3.4.4 Conclusions

i) The present work has shown that the slow strain rate SCC test is capable of distinguishing between the susceptibility to SCC of a typical Al-Zn-Mg alloy in different temper conditions.

ii) The characteristic decrease in susceptibility to SCC with overaging was observed for D74S.

iii) The higher ageing temperature in combination with shorter ageing times, produces superior SCC resistance, however, at the expense of considerable mechanical property loss.

iv) The PFZ width can be considered as an indication of the extent of the solute concentration profile developed at grain boundaries. During overageing a relationship exists between the PFZ width and resistance to SCC.

v) A moderate increase in resistance to SCC was observed with decreasing quench rate in D74S.

vi) The influence of small Cu-additions on the SCC susceptibility of Al-Zn-Mg alloys is explained in terms of a simple electrochemical model.

CHAPTER 4: FABRICATION, MECHANICAL AND PHYSICAL PROPERTY TESTING OF EXPERIMENTAL ALLOY COMPOSITIONS

4.1 Introduction

A major goal of the present investigation was the determination of the influence of both Zn and Mg content on the strength and SCC resistance of Al-Zn-Mg alloys. In order to isolate their effects, the transition elements Cr, Zr, and Cu, which markedly affect SCC properties were omitted from experimental compositions. A fibrous, unrecrystallised structure was, however, maintained in the fabricated plate by a 0.35% Mn addition. While this Mn content provides sufficient inhibition to recrystallisation (experimentally determined in Section 2.2.5) it will exert a minimal effect on strength and SCC properties (Figure 2.7). Grain refinement was achieved by Ti additions of approximately 0.020%.

Seven experimental alloy compositions were selected to provide a wide range of compositional variation. The intended compositions are represented by circles in Figure 4.1, which has been superimposed on Figure 2.2. It can be seen that alloys 1 and 2 are in Region I, alloy 3 is in Region II, alloys 4 and 7 are at the limits of Region III, and alloys 5 and 6 are in Region IV. In addition, it should be noted that alloys 2, 4 and

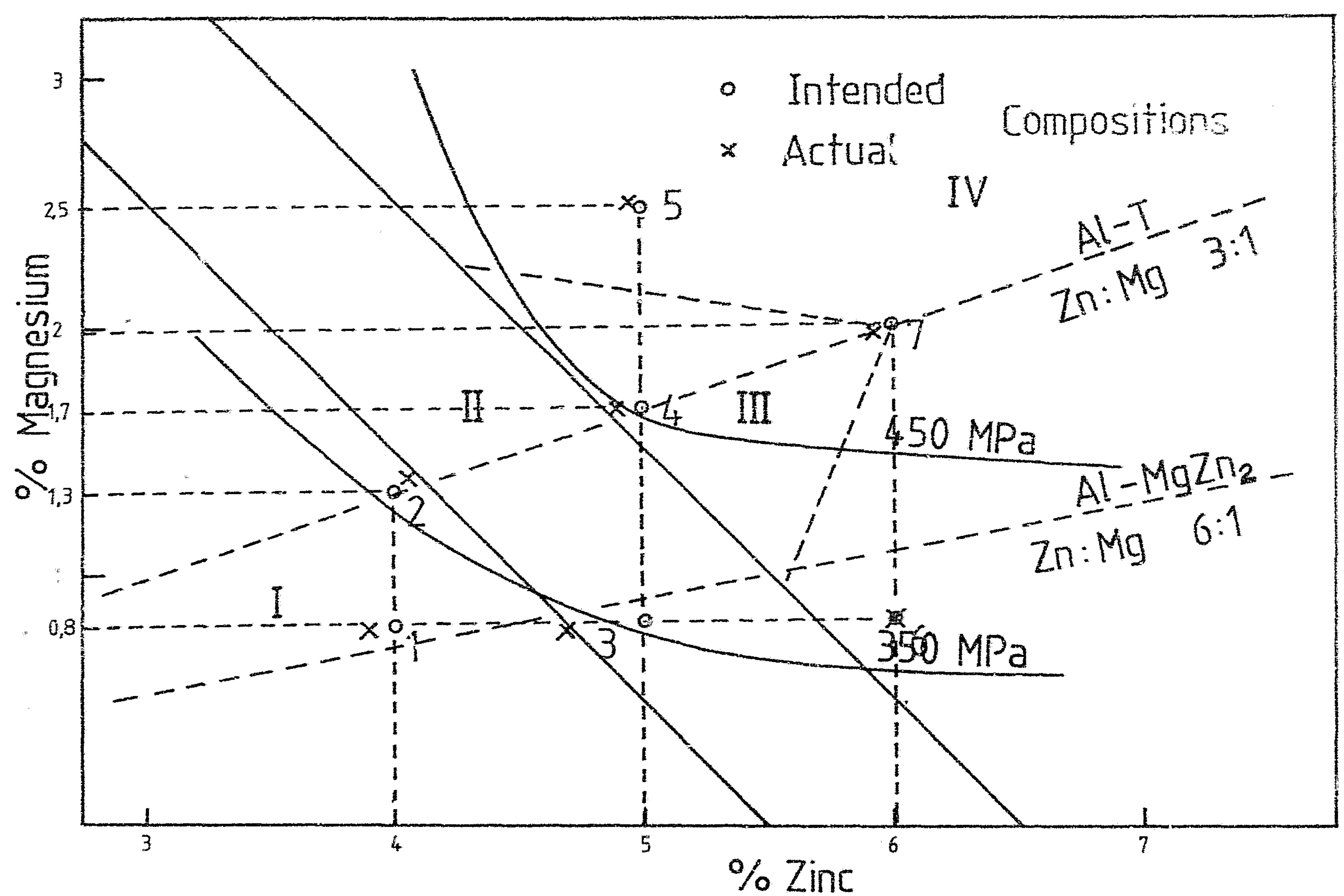

Figure 4.1 Schematic representation of experimental all...

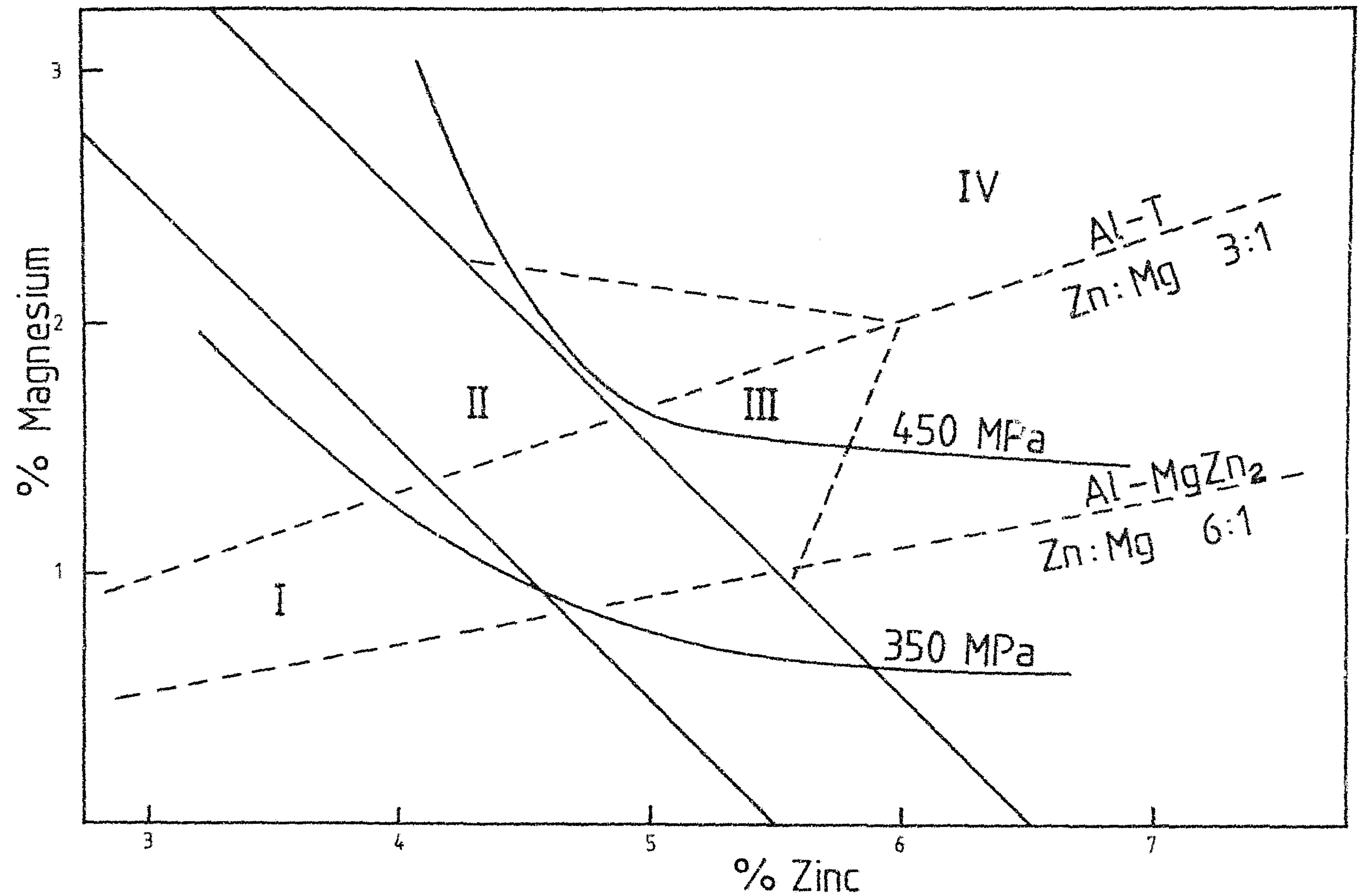

Figure 4.1 Schematic representation of experimental alloy compositions "O" represents intended compositions, "X" represents actual compositions.

7 have the optimum Zn : Mg ratio of 3 : 1 which has been reported to produce maximum resistance to SCC (See Section 2.2.1 (i)).

The alloys were cast and fabricated using techniques developed to reduce the ingot defect content. The material was heat treated and aged to a slightly overaged condition. Mechanical properties, and susceptibility to SCC using the slow strain rate test, were determined.

4.2 Casting, Fabrication and Heat Treatment

In order to produce experimental alloy ingots with a low defect content, it was necessray to develop a relatively sophisticated melting, casting and fabrication procedure. The harmful effects of ingot defects, particularly in the slow strain rate SCC testing of smooth specimens, produce unreliable results in at least 2 ways. Firstly, they can form stress corrosion crack nuclei, and secondly, they facilitate crack propogation[49,82]. It is essential, therefore, that these inherent flaws are kept to the lowest practical level.

The alloys were induction melted, using a coil fitted with a graphite-impregnated crucible of 10kg. capacity (Figure 4.2), in an enclosed chamber. Melting and casting could therefore be carried out using normal atmospheres, protective gas atmospheres or under vacuum. The melts were direct cast into a rectangular steel mould. 5kg. ingots were produced from commercial purity (99.85%) Al, Zn and Mg. Mn was added to the melt in the form of high purity flake, and Ti as Al-5% Ti-1% B hardener. At all times the temperature of the melt was maintained below 750°C in order to minimise the evaporation of Zn and Mg. The pouring temperature was 700°C.

Initial melting and casting into a rectangular steel mould (50 x 100 x 230 mm high) was performed under 1 atmosphere of argon. During the tensile testing of these alloys, however, premature fracture and the presence of cavities on the fracture surfaces were observed. A further optical metallographic study revealed the existence of 2 common ingot defects: non-metallic inclusions and a combination of shrinkage and gas porosity. The non-metallic inclusions, principally trapped oxides, were found to cause extensive surface cracking of the ingot during hot rolling (Figure 4.3). This operation was, in addition, unable to heal the porosity (Figure 4.4). Subsequent melting and casting was therefore performed under normal atmospheric conditions in order to facilitate the implementation of the following techniques.

The oxide inclusions are generated by fracture and detachment of the oxide skin formed on the interface between the molten metal and air. They are, however, insoluble in the liquid and may be removed by controlled stirring and skimming of the melt. As the induction

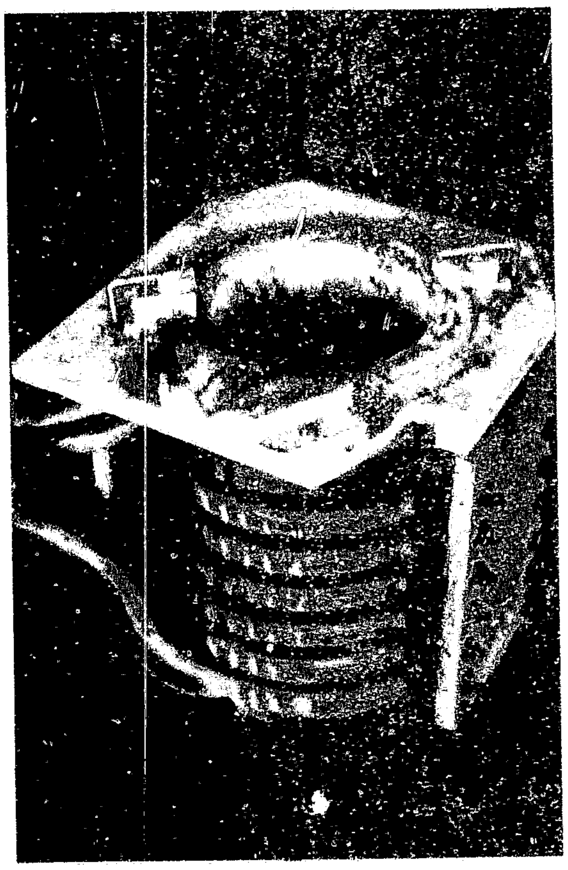

Figure 4.2 Induction furnace coil with graphite impregnated crucible (capacity 10 kg.)

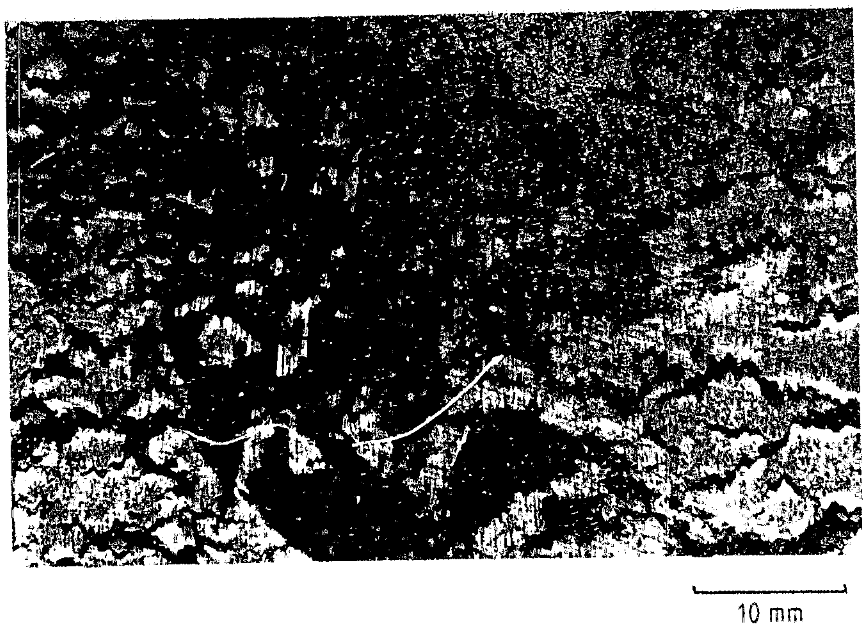

Figure 4.3 Extensive surface cracking produced during hot rolling.

field provides marked agitation of the melt a final skimming operation was performed immediately before casting in the absence of this field. During casting, remaining oxides and trapped non-metallic inclusions were further reduced by filtration. A woven glass-cloth filter sack was used which also reduced turbulence during the liquid metal transfer operation between furnace and mould.

Ingot porosity is particularly harmful when it remains unhealed in the final product (Figure 4.4). Solidification shrinkage, due to the large solidification range of Al-Zn-Mg alloys, is inevitable, usually resulting in centreline porosity. However, in the presence of hydrogen, the only gas which is soluble in the melt, the chances of healing porosity by the normal mechanism of pressure welding on hot working are reduced. It was therefore necessary to de-gas the melt. De-gassing was achieved by the mechanical scavenging effect of bubbling ultra-high purity nitrogen through the liquid metal for 30 seconds prior to casting using a gas-lance.

Shrinkage porosity may be reduced by:

a) encouraging directional solidification of the ingot; and
b) providing ample feeding during solidification.

An improved mould was therefore designed which would incorporate a "hot top" and reduce feeding distances. This design featured a rectangular mild steel mould (50 x 240 x 100 mm high) with a refractory feeding head (Figure 4.5). The mould was pre-heated to approximately 90°C to reduce the solidification rate and improve the surface quality of the ingot.

Ingots cast using the above techniques showed a marked reduction in ingot defects. A minimal amount of centreline shrinkage porosity was, however, observed after metallographic examination of the ingots. No cracking of the ingot developed during subsequent hot working (Figure 4.6).

The seven experimental alloys (Figure 4.1) were finally prepared using the above procedure. The ingots were homogenised for 12 hours at 470°C. A 2 mm thick section of the ingot surface was removed by scalping, which resulted in a 46 mm final thickness.

In order to ensure healing of the centreline porosity, the ingots were pre-forged at 450°C to a thickness of 28 mm. This process results in a greater uniformity of work through the ingot thickness (See Section 2.4.1). The forged ingots were subsequently re-heated to 450°C and hot-rolled to 12 mm plate. The minimum finishing temperature was 350°C. To achieve the total reduction, two re-heats during hot-rolling were required. The combined reduction of both hot working operations was 75%.

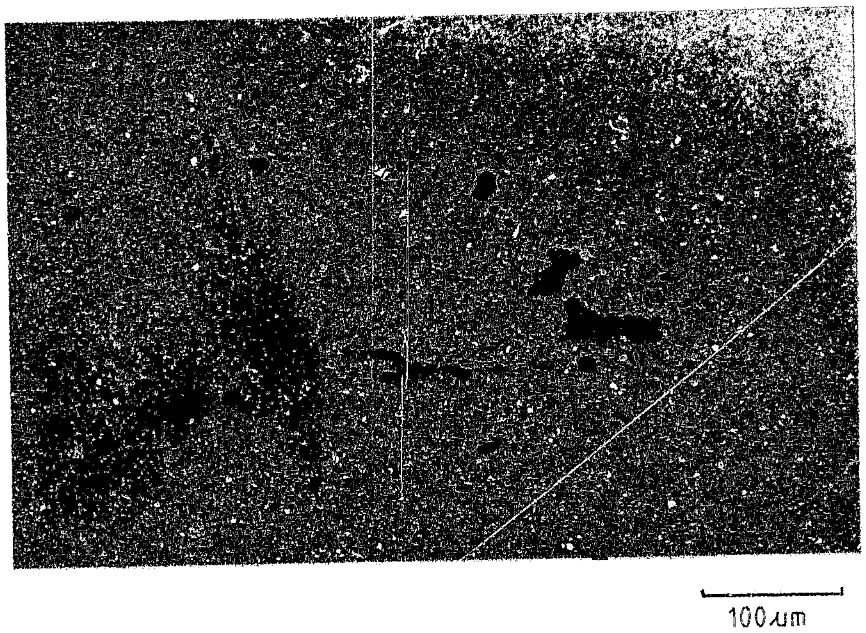

Figure 4.4 Unhealed porosity in experimental alloy plate after hot rolling.

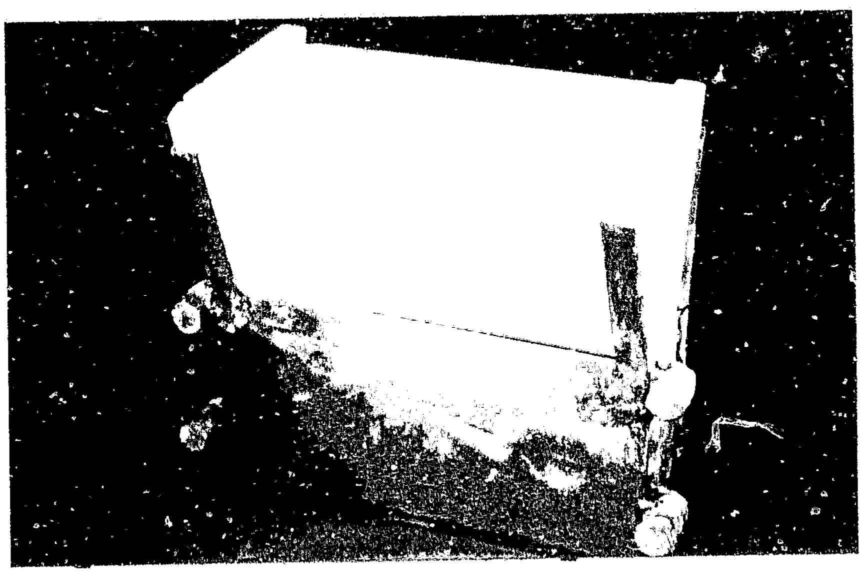

Figure 4.5 Ingot mould (capacity 5 kg)

Spectographic compositional analyses were obtained from each alloy and these results are presented in Table IX. A "LECO" hydrogen gas analysis was determined for each alloy and these are also shown in the Table.

Table IX: Experimental Alloy Compositions and Hydrogen Gas Contents

Alloy	Mg	Zn	Mn	Ti	Others	H_2 Content
					(Max.)	($ml.100g^{-1}$)
1	0.78	3.89	0.13	0.018	0.15	0.27
2	1.32	4.05	0.16	0.022	0.15	0.34
3	0.76	4.68	0.25	0.016	0.15	0.32
4	1.65	4.92	0.26	0.015	0.15	0.30
5	2.52	4.97	0.33	0.013	0.15	0.40
6	0.81	6.00	0.24	0.019	0.15	0.30
7	1.97	5.91	0.26	0.018	0.15	0.28

These compositions, which differ slightly in Zn and Mg contents from the intended compositions, are also shown in Figure 4.1 (as crosses).

The alloys were solution heat treated at 460°C for 2 hours and water quenched. This was immediately followed by a 90°C pre-age for 7 hours. The final ageing time required to peak-age Al-Zn-Mg alloys, is dependant on the (Zn + Mg) content. The time required to slightly overage the experimental alloys at 135°C was determined from Figure 2.14 (Section 2.2.5). The final ageing times for each alloy are shown in Table X.

Table X: Final Ageing Times at 135°C Required to Slightly Overage Experimental Alloys

Alloy	Final Ageing Time (hours)
1	36
2	28
3	28
4	26
5	24
6	28
7	24

4.3 Mechanical Property and SCC Testing

4.3.1 Experimental Procedure

An optical metallographic investigation was undertaken to determine the grain structure and grain size of the experimental alloys. Sections of each plate were polished and etched in 40% Tuckers reagent to reveal the extent of recrystallisation.

Tensile properties were determined in the longitudinal direction of each plate. Brinell hardness values were also obtained.

The susceptibility to SCC of each alloy was assessed using the slow strain rate test method (Section 3.3.3). Tests were performed in duplicate in the long transverse direction of each plate. Resistance to SCC was expressed as a ductility ratio using the reduction of area ductility parameter.

Exfoliation testing was conducted in accordance with the ASTM - G34 - 79 standard test method for exfoliation corrosion susceptibility (the EXCO test). The seven experimental alloys, together with the existing commercial base alloys D74S, D54S and B51S were evaluated to facilitate comparison.

4.3.2 Experimental Results

Optical examination of the grain structure revealed no evidence of recrystallisation. A fibrous grain structure was observed and a typical optical micrograph is shown in Figure 4.7. The grain size of each alloy was found to be comparable with that of D74S plate. Typical values obtained were:

Figure 4.6 Comparison of plate edges after hot-working. (a) Extensive cracking due to presence of non-metallic inclusions, and (b) after removal (by filtering) of these particles

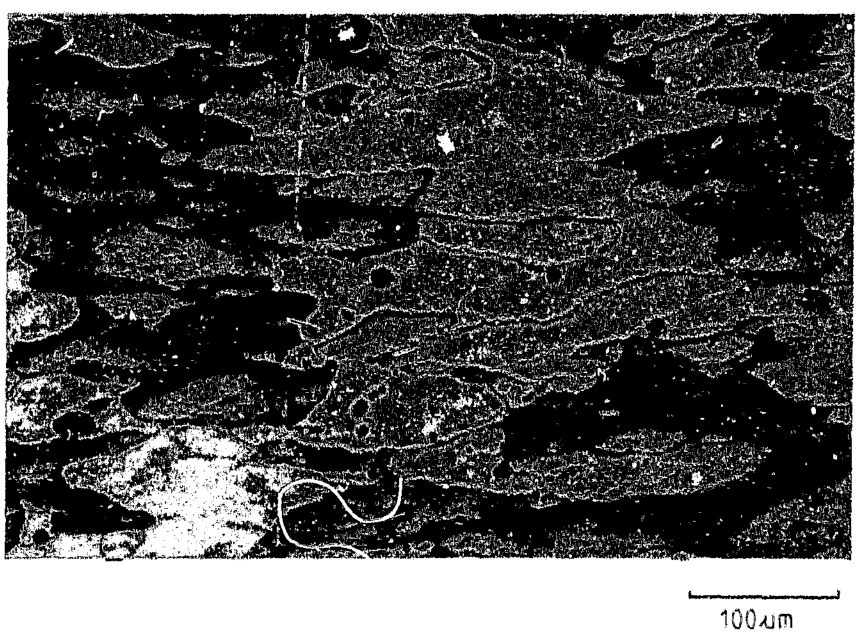

Figure 4.7 Typical optical micrograph slowing fibrous grain structure of experimental alloys.

Average longitudinal length - 220 μm ,

Average long transverse width - 200 μm ,

Average short transverse width - 57 μm .

The increased long transverse width is due to the forging operation.

Results of the tensile and hardness tests are presented in Table XI

Table XI: Tensile and Hardness Values for the Experimental Alloys

Alloy	0.2% Yield Stress (MPa)	Tensile Strength (MPa)	Elongation (%)	Hardness (Brinell)
1	229	278	20	102
2	316	355	17	129
3	290	326	23	126
4	410	430	21	142
5	447	480	20	167
6	328	357	24	128
7	468	480	16	131

It should be noted, however, that the strength of the dilute alloys 1 to 3 may be expected to increase with a natural ageing interval between quenching and pre-ageing.

The reduction of area ductility ratios obtained from slow strain rate testing, together with the (Zn + Mg) contents and Zn : Mg ratios for each alloy are presented in Table XII in order of decreasing susceptibility to SCC.

Table XII: Results of Slow Strain Rate Testing of Experimental Alloys shown together with the (Zn + Mg) Content and Zn : Mg Ratios

Alloy	(Zn + Mg)	Zn : Mg	Ductility Ratio
1	4.67	4.99	0.92
2	5.37	3.07	0.92
3	5.44	6.16	0.77
4	6.57	2.98	0.42
7	7.88	3.00	0.33
6	6.81	7.41	0.22
5	7.49	1.97	0.20

A comparison of susceptibility to SCC and tensile strength for each alloy composition is facilitated by plotting the ductility ratio versus the yield stress (Figure 4.8).

Exfoliation corrosion test results are presented in Table XIII in order of increasing severity. The visual ratings are in accordance with the classification used in ASTM - G34 - 79.

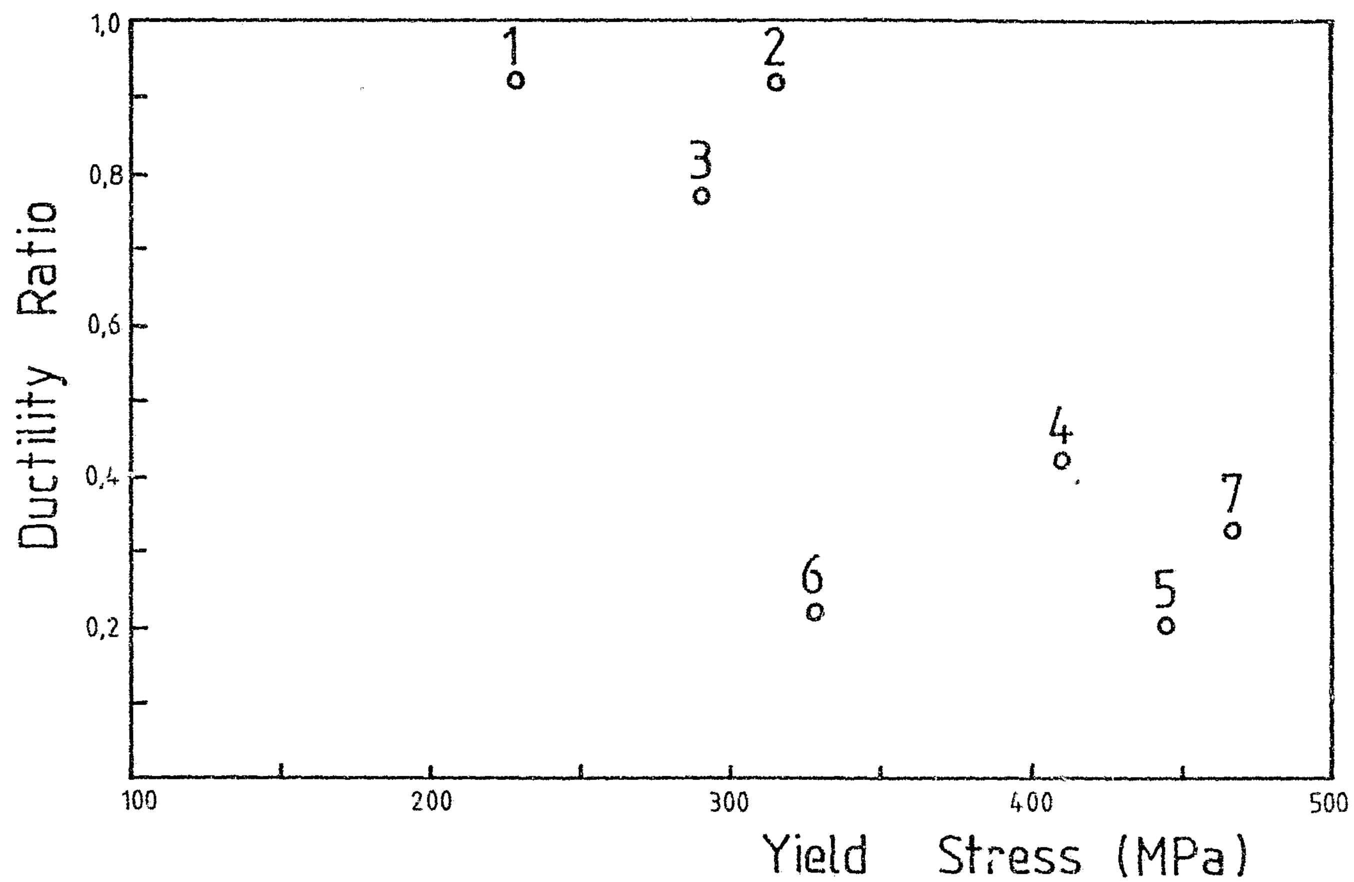

Figure 4.8 Schematic representation of the ductility ratio versus the Yield Stress for the seven experimental alloys.

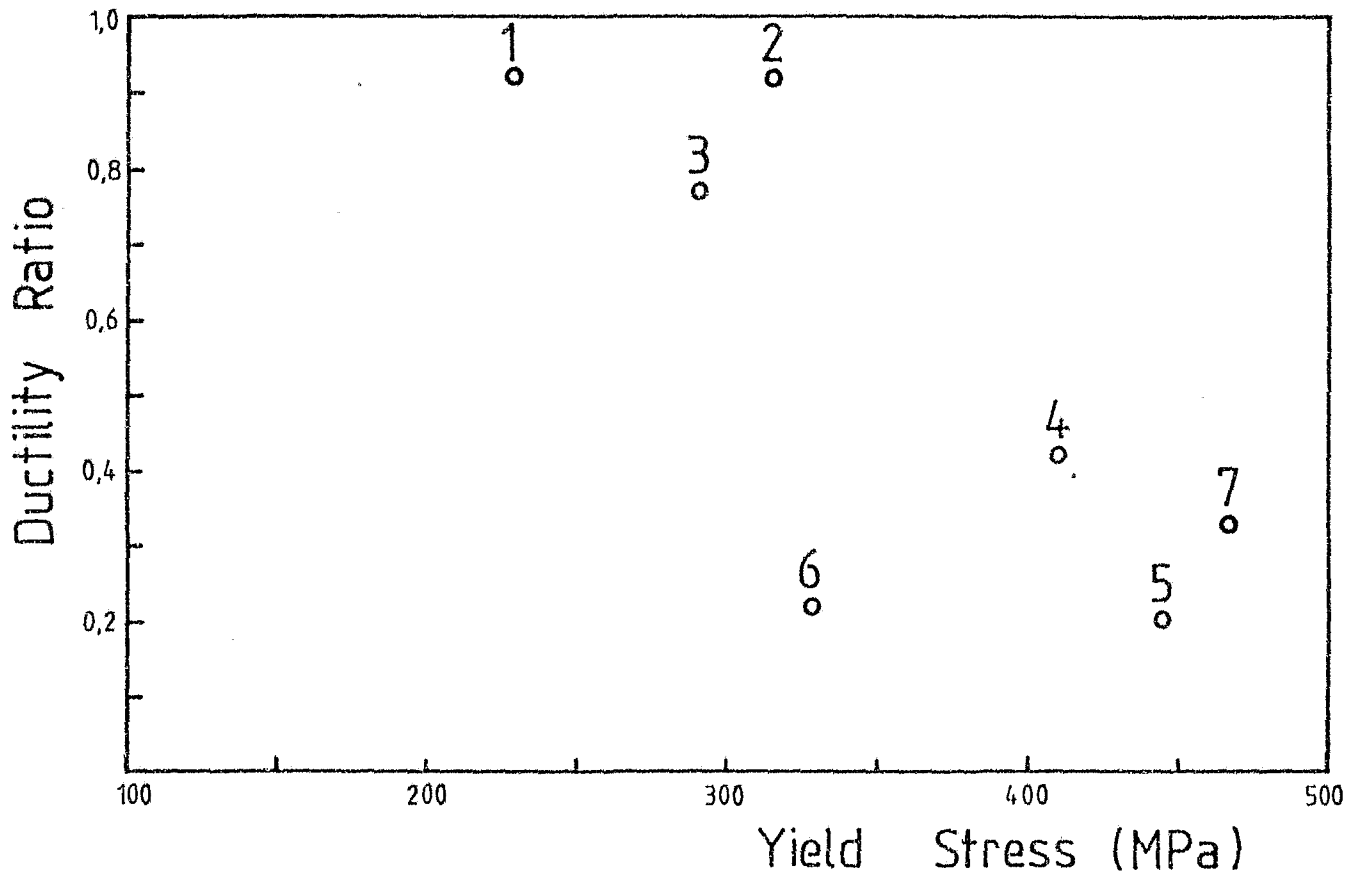

Figure 4.8 Schematic representation of the ductility ratio versus the Yield Stress for the seven experimental alloys.

Table XIII: Exfoliation Corrosion Ratings in order of Increasing Severity

Alloy and Temper	Rating and Comments
1 - slight overage	N - slight etching
2 - slight overage	N - slight etching
3 - slight overage	N - slight etching and pitting
6 - slight overage	N - slight etching
4 - slight overage	P - pitting and general corrosion
5 - slight overage	P - pitting and intergranular corrosion
7 - slight overage	P - pitting and intergranular corrosion
D54S - H2	P - severe pitting
B51S - T6	EA - superficial exfoliation
D74S - T6	EB - moderate exfoliation

In the Table: N indicates no appreciable attack; P indicates pitting; and EA to EB increasingly severe exfoliation corrosion.

Optical micrographs of the exfoliation surfaces after testing of the more severely corroded commercial alloys are shown in Figure 4.9.

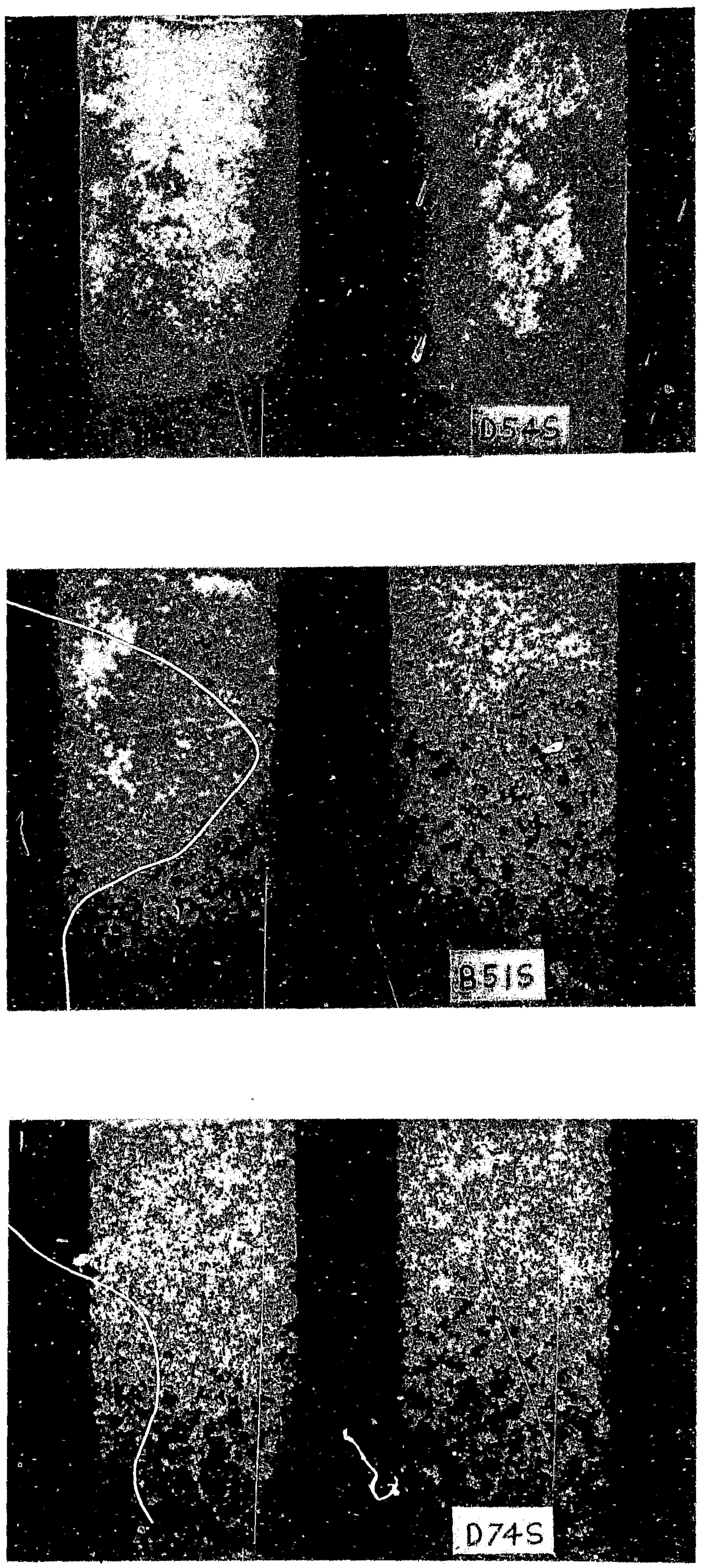

Figure 4.9

Optical micrographs showing exfoliation surfaces of the three commercial alloys

25mm

4.4 Discussion

Alloy compositions which have a Zn : Mg ratio of 3 : 1 have been reported to exhibit superior ageing response (Section 2.2.1 (ii)). This implies that the maximum strength is obtained for the least total solute content. In order to confirm this effect in the experimental alloy compositions reference should be made to Figure 4.10 in which the (Zn + Mg) content is plotted against the 0.2% yield stress. Alloys 2 and 3, 4 and 6, and to a lesser extent 5 and 7 have similar (Zn + Mg) contents. In each case it is apparent that the alloy with a Zn : Mg ratio of 3 : 1 (that is, alloys 2, 4 and 7) exhibits increased strength. It may therefore be concluded that over the compositional range covered by these alloys, the above Zn : Mg ratio does produce an optimum strength on ageing.

The effect of the Zn : Mg ratio on susceptibility to SCC may be deduced from Figure 4.8. Alloys 2, 3 and 6, and 5 and 7 exhibit similar yield strengths. However, in both cases alloys with a Zn : Mg ratio of 3 : 1 (that is, alloys 2 and 7) show improved resistance to SCC over alloys with similar strengths. For a given (Zn + Mg) content the same superiority of the optimum ratio alloys can be observed (Figure 4.11: compare alloys 2 and 3, 4 and 6, and 5 and 7). From the above considerations it is apparent that both optimum age-hardening and superior resistance to SCC may be obtained from alloy variations having a Zn : Mg ratio of 3 : 1.

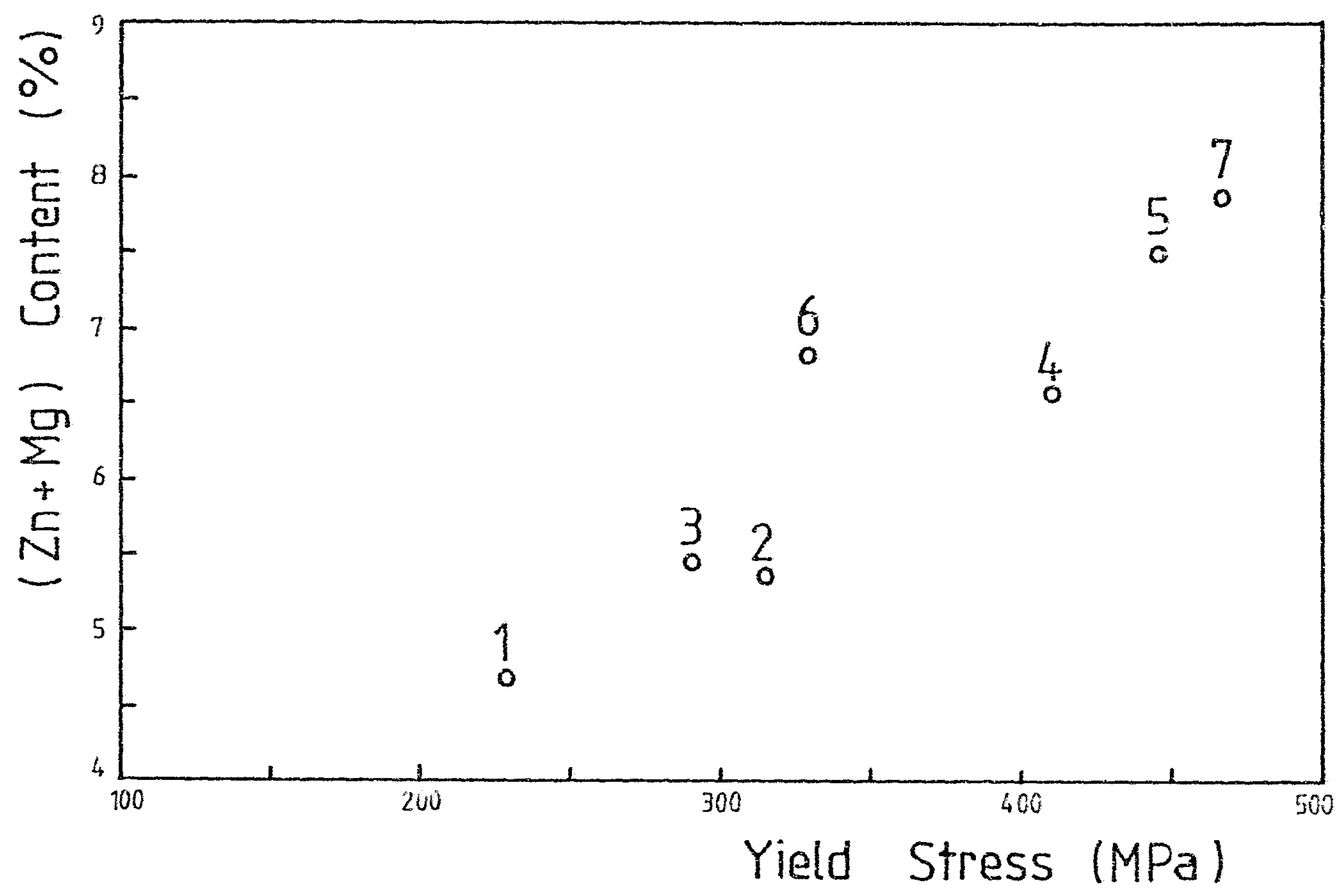

Figure 4.10 The (Zn + Mg) content of the experimental alloys is shown against the 0.2% yield stress

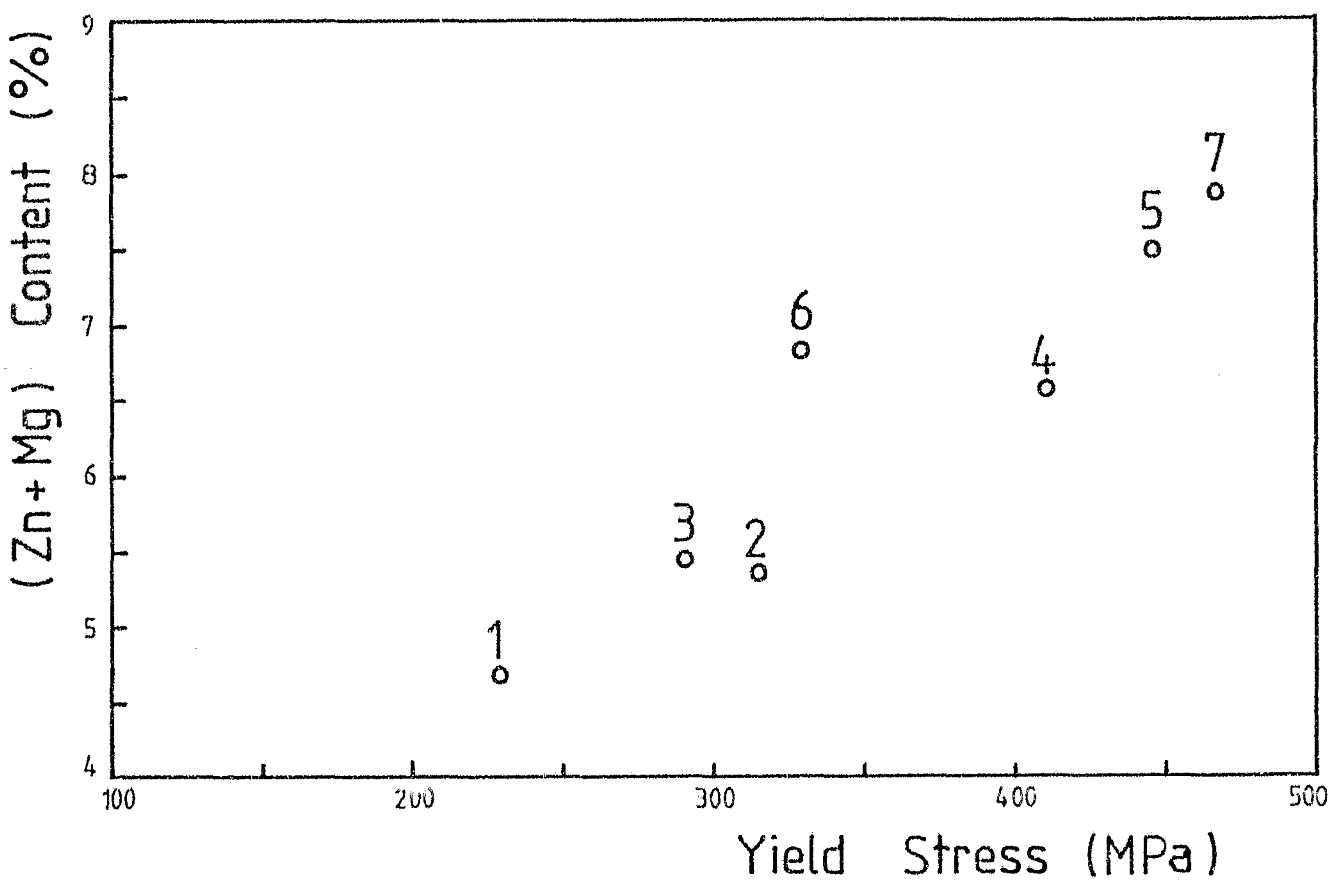

Figure 4.10 The (Zn + Mg) content of the experimental alloys is shown against the 0.2% yield stress

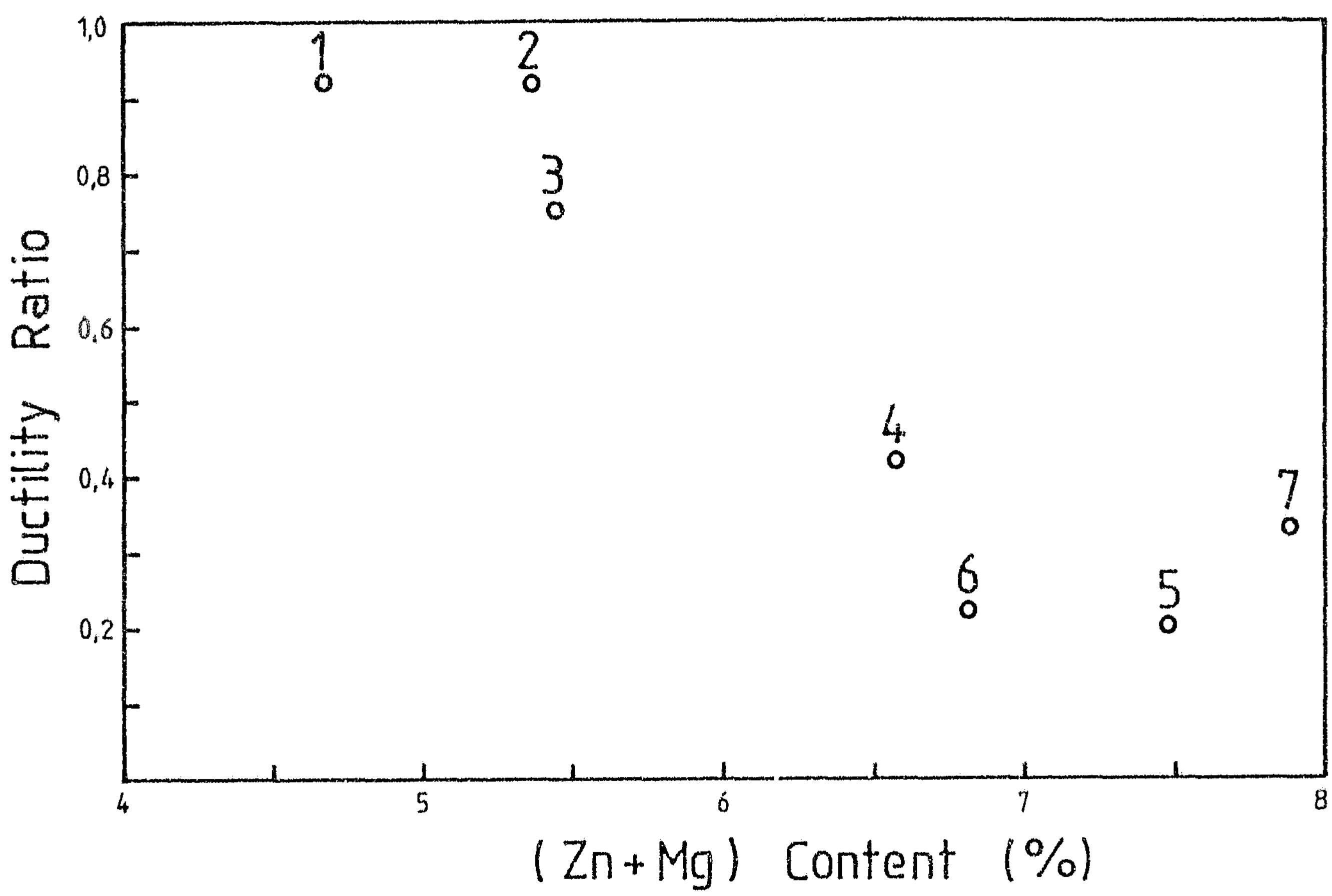

Figure 4.11 Schematic representation of the ductility ratio versus the (Zn +Mg) content for the seven experimental alloys.

A marked difference in exfoliation corrosion resistance between the experimental and commercial alloys is apparent in Table XIII. Two factors contribute to the improved performance of the experimental alloys.

1) The reduction during hot working of these alloys (75%) is considerably less than that of the commercial alloys ($\sim$95%). The grains in the experimental alloys therefore have a greater thickness to width ratio which leads to superior exfoliation resistance.

2) The experimental alloys were fabricated from high purity commercial stock and therefore have a reduced level of impurities and their related constituents. These phases provide weak regions at the surface oxide film, which promote electrochemical attack.

The exfoliation resistance of the experimental alloys appears to decrease with increasing (Zn + Mg) content. The ratings were not sufficiently sensitive to determine the effect of the Zn : Mg ratio.

4.5 Conclusions

i) In order to reduce the ingot defect content of small scale experimental alloy ingots, improved melting, casting and fabrication techniques were implemented.

ii) The mechanical properties were obtained for a number of base Al-Zn-Mg compositions. Optimum age-hardening response was exhibited by alloys with a Zn : Mg ratio of 3 : 1.

iii) Slow strain rate SCC testing of these alloys was also undertaken. The same Zn : Mg ratio was found to provide superior resistance to SCC.

iv) The exfoliation corrosion resistance of the experimental and three commercial alloys was evaluated using the EXCO test. Exfoliation was found to increase with an increasing (Zn + Mg) content.

CHAPTER 5: SUMMARY AND FUTURE WORK

In the course of the present investigation a sound metallurgical basis has been provided to facilitate further development of Al-Zn-Mg alloys with superior combinations of mechanical properties and SCC resistance. Background to the metallurgy and SCC of this alloy system was obtained by a comprehensive literature review. Particular attention was given to the reported influence of composition and heat treatment on microstructural features (e.g. PFZ, solute concentration profiles at grain boundaries, etc.) and SCC properties.

A suitable procedure for the rapid evaluation of SCC resistance was obtained by evaluating a number of accelerated test methods. The slow strain rate test was selected and subsequently shown to provide results consistent with the expected susceptibility to SCC of the alloys and their temper conditions.

A microstructural study of the repres ntative Al-Zn-Mg alloy, D74S, was undertaken. In addition, the effects of heat treatment variables on both microstructural features and the SCC resistance was investigated. This study revealed a relationship between susceptibility to SCC and the variation of the PFZ width during final ageing. A model for the observed relationship was proposed in which the PFZ width is considered as an indication of the extent of the solute profile at the grain boundaries. The apparent absence of a similar relationship between SCC resistance and the increasing PFZ width with decreasing quench rate was explained in terms of the same model.

The tensile and SCC properties of seven Al-Zn-Mg alloy compositions were determined. The alloys were selected to cover a wide compositional variation (Zn: 4 - 6%, Mg: 0.8 - 2.5%). Melting, casting and hot working techniques were developed to provide defect-free experimental-scale ingots. In particular, methods to reduce non-metallic inclusions as well as gas and shrinkage porosity were employed. Results of tensile and slow strain rate SCC testing revealed the beneficial effects of a Zn : Mg ratio of 3 : 1. Compositional variations with this ratio showed superior age-hardening response and resistance to SCC.

The present project formed part of a comprehensive alloy development programme to replace the existing commercial alloys D74S, D54S and B51S with improved medium to high strength, weldable Al-Zn-Mg alloys. The two compositions Al-5Zn-1.7Mg and Al-6Zn-2Mg were shown in Chapter 4 to provide a combination of both the required tensile strength and superior SCC resistance. They will therefore form the base compositions for further investigations.

Recommendations for future work were identified and include the following:

1) A detailed assessment of the effects of transition element additions on both mechanical and SCC properties. The influence of Cr, Zr and (Cr + Zr) additions, alone or in the presence of a small Cu addition, should receive particular attention.

2) A determination of the effects of heat treatments on the properties of the most promising alloys, by:

   i) a study of conventional heat treatments and conditions, such as:

      a) the heating rate to homogenisation (in the presence of Zr),
      b) the homogenisation time and temperature,
      c) the SHT time and temperature (particularly with regard to the extent of recrystallisation produced during this treatment),
      d) the quench rate (particularly the effect of minor transition additions on quench sensitivity),
      e) ageing time and temperature; and

   ii) an investigation of the effects of step quenching techniques on both mechanical properties and SCC resistance (particularly with regard to quenching from the hot mill), and finally;

iii) a detailed investigation of the retrogressive reageing (RR) technique.

3) A correlation of the slow strain rate test data with existing long term SCC test methods. (For example, this work has revealed a relationship between PFZ width (after different ageing times) and susceptibility to SCC. Other workers have shown a similar relationship to exist using C-ring SCC test results. It therefore appears that a relationship between slow strain rate and C-ring test data should exist). This will hopefully lead to a more meaningful prediction of alloy performance in service, from the slow strain rate test results.

4) An investigation of the influence of composition (particularly small Cu additions) and heat treatment on the exfoliation corrosion resistance.

Further investigations will necessarily involve extensive mechanical property determiniation, SCC evaluation and a detailed microstructural study of experimental compositions. The aim should be not only to develop a superior composition and heat treatment schedule but also to understand the mechanisms involved. With a greater emphasis placed on a mechanistic approach further progress and manipulations of these alloys will be more easily facilitated.

REFERENCES

1) I J Polmear : Light Alloys - (Metallurgy and Materials Science), R W K Honeycombe and P Hancock, eds., Edward Arnold, London, 1981.

2) K R Van Horn, ed. : Aluminium, vol. I, ASM, Metals Park, Ohio, 1967.

3) M Van Lancker : Metallurgy of Aluminium Alloys, Chapman and Hall, London, 1967.

4) M V Hyatt and M O Speidel : Stress Corrosion Cracking in High Strength Steels and in Titanium and Aluminium Alloys, p.147, Naval Res. Lab., Washington, 1972.

5) M O Speidel and M V Hyatt : Advances in Corrosion Science and Technology, vol. 2, p.115, Plenum Press, New York, 1972.

6) L F Mondolfo : Metals and Materials, 1971, vol. 5, p.95.

7) M O Speidel : The Theory of Stress Corrosion Cracking in Alloys, J C Scully, ed., NATO Conference, 1971.

8) A W Thompson and I M Bernstein : Stress Corrosion Cracking, J Yahalom and A Aladjem, eds., p.193, Freund, Switzerland, 1980.

9) G M Scamans : Notes on the Stress Corrosion Cracking of Weldable Al-Zn-Mg Alloys, Alcan Extrusions Technical Seminar on Strong Alloys, Canada, 24-25 Nov. 1981.

10) H Cordier, C Dumont, W Gruhl : Metall. 34, 1980, no. 6, p.515.

11) A T Thomas, A J Bryant : Effect of Composition and Solution Treatment Conditions on Tensile and Impact Properties of Al-Zn-Mg Alloy Sheet, Alcan Research and Development Report, B - RR - 1106, 1969, unpublished.

12) W Gruhl : The Stress-Corrosion Behaviour of High-Strength at Al-Zn-Mg Alloys, Aluminium Alloys in the Aircraft Industry, p.171, Assoiciazione Italiana Metallurgica and the Instituto Sperimentale dei Metalli Seggeri, Technicopy Ltd., England, 1976.

13) H Westengen, O Reiso, L Auran : Aluminium 56, 1980, p.768.

14) M V Hyatt : New Aluminium Aircraft Alloys for the 1980's, Aluminium Alloys in the Aircraft Industry, p.31, Associazione Italiana Metallurgica and the Instituto Sperimentale dei Metalli Seggeri, Technicopy Ltd., England, 1976.

15) H Cordier, C Dumont, W Gruhl, B Grzemba : Metall. 36, 1982, p.33.

16) B Sarkar, M Marck, E A Starke, Jr. : Met. Trans. A, 1981, vol. 12A, p.1939.

17) W Gruhl, M Schippers : Z. Metallkunde 58, 1976, p.679.

18) G Scharf : Aluminium 45, 1969, p.150.

19) W M Bell : Metallurgy of the Press Quenchable Al-Zn-Mg Alloys, Hulett Aluminium Internal Report, South Africa, 1979.

20) H Westengen, L Auran, O Reiso : Aluminium 57, 1981, p.797.

21) M O Speidel : The Theory of Stress Corrosion Cracking in Alloys, J C Scully, ed., p.289, NATO, Brussells, 1971.

22) D E Ward, G W Lorimer : Stress Corrosion in Aluminium Alloys, Fifth Report on Agreement No. AT/2052/025 MAT, University of Manchester, Manchester, 1974.

23) B D Warr, G W Delamore, R W Smith : Met. Trans. B, 1975, vol. 6B, p.625.

24) M Atkinson, J V Bee : Effect of Minor Additions of Chromium and Zirconium on the Microstructure of a Hot Worked Al-Zn-Mg Alloy, Dept. of Metallurgy, University of the Witwatersrand, 1982.

25) J D Embury, R B Nicholson : Acta Met., 1965, vol. 13, p.403.

26) H Irone, T Sato, Y Kojima, T Takakashi : Met. Trans. A, 1981, vol. 12A, p.1429.

27) T Ungar : Z. Metallkde., 1979, vol. 70, p.739.

28) H P Degischer, W Lacom, A Zahra, C V Zahra : Z. Metallkde., 1980, vol. 71, p.231.

29) J M Papazian : Met. Trans. A, 1982, vol. 13A, p.761.

30) J Lendvai, G Y Honyck, I Kovacs : Scripta Met., 1979, vol. 13, p.593.

31) J Gjonnes, Chr. J Simensen : Acta Met., 1970, vol. 18, p.881

32) P E Roper, J W Martin : Z. Metallkde., 1979, vol. 70, p.401.

33) J Lendvai, I Kovacs, T Ungar, J Lakner, K Banizs : Aluminium, 1980, vol. 56, p.453.

34) A Zahra, C V Zahra, M Laffitte, W Lacom, H P Degischer : Z Metallkde., 1979, vol. 70, p.172.

35) C M Wan, W Y Wei, M T Jahn : J. of Mat. Science, 1981, vol. 16, p.1097.

36) H J McQueen : Thermomechanical Processing of Aluminium Alloys, J G Morris, ed., p.1, TMS - AIME, Warrendale, 1979.

37) D M Van Der Walker, J B Van Der Sande : Met. Trans. A, 1981, vol. 12A, p.1787.

38) R Gronsky, P Furrer : Met. Trans. A, 1981, vol. 12A, p.121.

39) A T Thomas, A J Bryant : Relation Between Grain Structure and Quench Sensitivity of A74S, Alcan Banbury Research and Development Report, B - RR - 1110, 1969, unpublished.

40) Y Miyagi, M Hirano : The Effect of Heat Treatment on Stress Corrosion Cracking of Al-Zn-Mg Alloy, Kobelco Technical Bulletin - 1007/1980, Kobe Steel Ltd., 1980.

41) M Raghavan : Met. Trans. A, 1980, vol. 11A, p.993.

42) R K Viswanadham, T S Sun, J A S Green : Met. Trans. A, 1980, vol. 11A, p.85.

43) A Joshi, C R Shastry, M Levy : Met. Trans. A, 1981, vol. 12A, p.1081.

44) P Doig, J W Edington : Br. Corros. J. (Quarterly), 1974, vol. 9, p.220.

45) D E Ward, G W Lorimer : Stress Corrosion in Aluminium Alloys, Fifth Report on Agreement No. AT/2052/025 MAT, University of Manchester, Manchester, 1974.

46) T Anthony : Acta Met., 1969, vol. 17, p.603.

47) T F Bower, D A Granger, J Keverian : Solidification, p.385, ASM, Metals Park, Ohio, 1970.

48) R E Reed-Hill : Physical Metallurgy Principles, 2nd. ed., p.602, D Van Nostrand Company, New York, 1973.

49) A J Bryant : Metallurgical Factors Affecting the Control of Mechanical Properties in High-Strength Aluminium Alloys, Aluminium Alloys in the Aircraft Industry, p.45, Associazione Italiana Metallurgica and the Instituto Sperimentale dei Metalli Leggeri, Technicopy Ltd., England, 1976.

50) A Thomas : Procedings of 6th International Conference on Light Metals, Leoben, Austria, Aluminium - Verlag, Dusseldorf, 1975.

51) A J Bryant, H J Lamb : Effect of Solution Heat Treatment Time and Temperature on Solute Solubility in Al-Zn-Mg Alloys, Alcan Banbury Research and Development Report, B - RR - 1117, 1969, unpublished.

52) H Bischel : Aluminium, 1973, vol. 49, p.477.

53) M O Speidel, M D Hyatt : Advances in Corrosion Science and Technology, vol. 2, M G Fontana, R W Stackle, eds., Plenum Press, New York, 1972.

54) C R Shastry, G Judd : Met. Trans. A, 1972, vol. 3, p.779.

55) A J Bryant : Ageing Characteristics of Extruded Al-Zn-Mg Alloys, Alcan Banbury Research and Development Progress Report No. 9, B - RR - 1002, 1967, unpublished.

56) J Lendvai, I Kovacs, T Ungar, J Lakner, K Barizs : Aluminium, 1980, vol. 56, p.453.

57) A J Bryant : Hardness-Time Ageing Characteristics of Alloys Containing 3.5 - 5.0% Zn and 1,0 - 1,7% Mg, Alcan Banbury Research and Development Progress Report No. 7, B - RR - 1002, 1967, unpublished.

58) L Ratke, W Gruhl : Z Metallkde,. 1980, vol. 9, p.568.

59) P D Hess : Light Metals, p.591, AIME, N Y, 1974.

60) R Alani, P R Swann : Br. Coros. J., 1977, vol. 12, No. 2, p.80.

61) R S Pathania, D Tromans : Met. Trans. A, 1981, vol. 12A, p.607.

62) D Hardie, N J H Holroyd, R N Parkins : Metal Science, 1979, Nov., p.603.

63) N J H Holroyd, D Hardie : Corrosion Science, 1981, vol. 21, p.129.

64) N J H Holroyd, D Hardie : Hydrogen Effects in Metal, Conference Proceedings, I M Bernstein, A W Thompson, eds., TMS - AIME, 1980.

65) J Kruger : Failure by Stress Corrosion Cracking, Stress Corrosion Cracking, J Yahalom, A Aladjem, eds., Freund, Switzerland, 1980.

66) P Doig, J W Edington : Corrosion - NACE, 1975, vol. 31, No. 10, p.347.

67) P Doig, P E J Flewitt, J W Edington : Corrosion - NACE, 1977, vol. 33, No. 6, p.217.

68) A J Jacobs : T.A.S.M., 1965, vol. 58, p.579.

69) A J De Ards, R Townsend : Met. Trans., 1970, vol. 1, p.2573.

70) B Cina, B Ranish : Aluminium Industrial Products, A.S.M., Golden Triangle, Pittsburgh, 1974.

71) B Cina, B Ranish : US Patent 3856584, Dec. 24, 1974.

72) B Cina : 2nd Israel - Norwegian Technical and Scientific Symposium Electrochemistry - Corrosion, The Norwegian Institute of Technology, Trondheim, Norway, 1978.

73) W Wallace, J C Beddoes, M C deMalherbe : Canadian Aero and Space J., 1981, vol. 27, No. 3, p.223.

74) R E Swanson, I M Bernstein : Scripta Met., 1982, vol. 16, p.321.

75) J Brettle, S Orman : Anti-Corrosion, 1973, Sep. p.3.

76) G M Scamans : Slow Strain Rate Stress - Corrosion Testing of Aluminium Alloys, Alcan Laboratories Ltd, Banbury Research and Development Centre, Report of Meeting held 20 March 1980.

77) G M Scamans : Aluminium, 1981, vol. 4, p.269.

78) J M Silcock : Corr. Science, 1981, vol. 21, p.723.

79) N J H Holroyd, G M Scamans : Draft of Paper Submitted to ASTM Symposium on Environment-Sensitive Fracture : Evaluation and Comparison, April 26-28, 1982, National Bureau of Standards, Washington D.C., USA.

80) Minutes of 2nd Meeting of the European Aluminium Association Working Party: Slow Strain Rate Stress-Corrosion Testing of Aluminium Alloys, Leichmetall - Forschungsinstitut Vereinigte Aluminium - Werker A.G., Bonn, May 1982.

81) Minutes of 3rd Meeting of the EAA Working Party : Slow Strain Rate Stress Corrosion Testing of Aluminium Alloys, European Aluminium Association Office, Dusseldorf, Oct. 1982.

82) N J H Holroyd, D Hardie : Metals Tech., 1982, vol. 9, p.229.

APPENDIX

The nominal chemical compositions of the three different existing base alloys: D74S, D54S, and B51S are presented in Table A1. In addition, typical tensile properties of the various commercial temper conditions are presented in Table A2. The alloys were supplied by Hulett Aluminium Ltd in the form of 12 mm plate.

Table A1: Chemical Compositions of Commercial Alloys

ALLOY	Cu	Fe	Mg	Mn	Si	Ti	Zn	Cr	Others	
									Each	Total
D74S	0.25 Max	0.4 Max	1.0 1.5	0.2 0.7	0.4 Max	0.1 Max	3.8 4.8	0.25 Max	0.05	0.15 Max
D54S	0.10 Max	0.4 Max	4.0 4.9	0.5 1.0	0.4 Max	0.2 Max	0.2 Max	0.25 Max	0.15	0.15 Max
B51S	0.10 Max	0.5 Max	0.5 1.2	0.4 1.0	0.7 1.3	0.2 Max	0.2 Max	0.25 Max	0.05	0.15 Max

Table A2: Typical Tensile Properties for Some Commercial Tempers

Alloy	Temper	0.2% Yield Stress (MPa)	Tensile Strength (MPa)	% Elongation
D74S	SHT and aged	330	360	11
D54S	as extruded	200	315	16
B51S	SHT, drawn and aged	315	330	10